

Review

# Recent Progress on Solid Substrates for Surface-Enhanced Raman Spectroscopy Analysis

Kun Ge, Yuling Hu \*  and Gongke Li 

School of Chemistry, Sun Yat-sen University, Guangzhou 510006, China

\* Correspondence: ceshyl@mail.sysu.edu.cn

**Abstract:** Surface-enhanced Raman spectroscopy (SERS) is a powerful vibrational spectroscopy technique with distinguished features of non-destructivity, ultra-sensitivity, rapidity, and fingerprint characteristics for analysis and sensors. The SERS signals are mainly dependent on the engineering of high-quality substrates. Recently, solid SERS substrates with diverse forms have been attracting increasing attention due to their promising features, including dense hot spot, high stability, controllable morphology, and convenient portability. Here, we comprehensively review the recent advances made in the field of solid SERS substrates, including their common fabrication methods, basic categories, main features, and representative applications, respectively. Firstly, the main categories of solid SERS substrates, mainly including membrane substrate, self-assembled substrate, chip substrate, magnetic solid substrate, and other solid substrate, are introduced in detail, as well as corresponding construction strategies and main features. Secondly, the typical applications of solid SERS substrates in bio-analysis, food safety analysis, environment analysis, and other analyses are briefly reviewed. Finally, the challenges and perspectives of solid SERS substrates, including analytical performance improvement and largescale production level enhancement, are proposed.

**Keywords:** surface-enhanced Raman spectroscopy; solid substrate; construction; applications; perspectives



**Citation:** Ge, K.; Hu, Y.; Li, G. Recent Progress on Solid Substrates for Surface-Enhanced Raman Spectroscopy Analysis. *Biosensors* **2022**, *12*, 941. <https://doi.org/10.3390/bios12110941>

Received: 14 October 2022

Accepted: 27 October 2022

Published: 30 October 2022

**Publisher's Note:** MDPI stays neutral with regard to jurisdictional claims in published maps and institutional affiliations.



**Copyright:** © 2022 by the authors. Licensee MDPI, Basel, Switzerland. This article is an open access article distributed under the terms and conditions of the Creative Commons Attribution (CC BY) license (<https://creativecommons.org/licenses/by/4.0/>).

## 1. Introduction

Surface-enhanced Raman spectroscopy (SERS) has emerged as a powerful and useful vibrational spectroscopy analytical technique with unique superiorities in terms of non-destructivity, ultra-sensitivity, rapidity and fingerprint features [1]. With the rapid development of SERS substrates in recent years, SERS has achieved obvious achievements in several fields, including chemical [2], food [3], environment [4], and biological analysis [5]. In general, the original Raman signals of analytes are inherently weak on account of the smaller Raman scattering cross-sections, indicating the irreplaceable role of substrates in boosting Raman signals [6]. In general, the enhancement mechanisms, including electromagnetic (EM) and chemical (CM) enhancement, can be used to enlarge the Raman signals. For EM, when the frequency of incident is in resonance with the frequency of localized surface plasmon on the surface of metal, the incident electric field can be amplitude, as well as the Raman signals of molecules absorbed on the surface of metal [7]. For CM, the charge transfer (CT) between the substrates and molecules can enlarge the Raman cross-section of molecules, leading to higher Raman signals [8]. The noble metal nanoparticles (gold, silver, copper, etc.) are widely used due to their ideal SERS signal enhancement and simple preparation process [9]. However, the SERS performance of molecules, including sensitivity and stability induced by metallic colloids, mainly relies on the aggregation state of metal nanoparticles, this necessitating a gentle detection environment and improvement of molecule–metal interactions [10]. Therefore, several matrixes, including SiO<sub>2</sub> or Al<sub>2</sub>O<sub>3</sub> [11], polymers [12], metal-organic frameworks (MOFs) [13,14], semiconductor [15,16], and carbon materials [17,18], have been applied to combine with

noble metal nanoparticles to improve the inherent instability of metallic colloids in SERS analysis. However, the development of high-quality substrates to generate sensitive and stable SERS signals can also be achieved through changing the form of substrate. In the past few years, more and more substrates with solid form, namely solid SERS substrates, have been developed due to their promising sensitivity, high stability, controllable morphology, and convenient portability. The fabrication of solid SERS substrates provides a promising strategy to improve the SERS performance in terms of stability, sensitivity, and portability.

Solid SERS substrates represent a special class of SERS substrate with solid features compared to colloid substrates. The general SERS measurements based on liquid substrates will meet limitations in terms of unstable signals, lower SERS activity, and short storage time. The solid SERS substrates show significant features in several aspects: (1) various preparation methods, including filtration, spin coating, chemical vapor deposition, magnetron sputtering, and self-assembly, are available for the fabrication of solid SERS substrates; (2) highly dense hot spots originating from concentrated unit area confirm the high SERS signals; (3) controllable micro morphology and structure, as well as good repeatability and reproducibility, provide uniform and stable SERS signals; (4) the solid features can significantly improve the stability of Raman signals to expand the scope of SERS analysis in practical applications, especially in reducing the requirement for sample pretreatment. Considering several superiorities of solid substrates in practical SERS analysis, the engineering of high-quality solid SERS substrates can significantly improve the analytical performance for SERS analysis.

In this paper, we comprehensively summarize the recent advances made in the field of solid SERS substrates for SERS analysis in the last five years (2017–2022). The main content of this review can be briefly described in Figure 1. Firstly, the common construction methods for solid SERS substrates are briefly introduced. Secondly, the main categories of solid SERS substrates, including membrane substrate, self-assembled substrate, chip substrate, magnetic substrate, and other solid substrate, were reviewed systematically. Then, the representative analysis applications in several fields, such as bio-analysis, food safety analysis, environment analysis, and other analyses, are introduced. Finally, the challenges and perspectives of solid SERS substrates for SERS analysis, including analytical performance improvement and sample pretreatment capability enhancement, are proposed. We sincerely hope that this review can help and inspire more researchers in developing useful solid substrates for SERS analysis with high analytical performance.

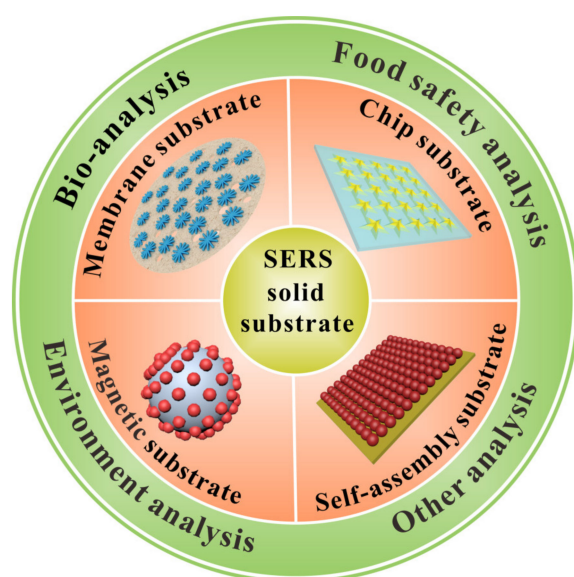


**Figure 1.** Various solid SERS substrates employed in analytical applications.

## 2. Common Construction Methods

The solid SERS substrates can be fabricated by immobilization technologies, mainly including printing/writing, filtration, self-assembly, spin coating, magnetron sputtering, surface modification, deposition, in-situ grown, and immersion, etc. Printing/writing is a traditional technology with metallic colloids as inks, exhibiting unique features in terms of low cost, simplicity, and great potential for largescale production to support the fabrication of membrane/chip substrates [19,20]. However, the instability of metallic colloids over time and single material source limit their commercialization. Filtration has been widely used to fabrication of paper membrane substrates due to its low cost, simplicity, potentials in largescale production and abundant available materials [21,22]. In general, the materials can be trapped by cellulose-based paper matrix with unique spatial reticular structure under external forces. The stability of paper membrane substrates over time can be improved by using plasmon-free materials compared to printing substrates [23,24]. The construction of solid SERS substrates by self-assembly method with controllable morphology, uniform and dense distributions of “hot spot” can be realized under three-phase system (water-ethanol-cyclohexane/hexane/chloroform) combined with drying-mediated self-assembly mechanism [25–27]. In addition, some chemical inert template supports, including polystyrene spheres (PS), SiO<sub>2</sub>, and melamine-formaldehyde (MF), can significantly extend storage time compared to pure metallic colloids [28–30]. Spin coating is a simple and effective method for the fabrication of solid SERS substrates. The colloidal solution containing materials was sputtered onto the surface of solid supports at a certain speed, confirming the tight and uniform distribution of materials [31,32]. The various available materials and solid supports endow such materials with great potential in terms of commercialization for the fabrication of solid SERS substrates by the spin coating method. Magnetron sputtering is an effective method belonging to physical vapor deposition (PVD). The electrons will bombard targets under the interaction between magnetic field and electric field, resulting in the sputtering of targets on the surface of solid supports. The uniformity and thickness of targets can be controlled through sputtering voltage, pressure, and time [33,34]. The magnetron sputtering provides an efficient and mechanized fabrication method for solid SERS substrates, exhibiting great potential in terms of largescale production. However, the high cost of magnetron sputtering instruments and targets limits their commercialization process. Surface modification is a traditional fabrication method for solid SERS substrates, which is mainly dependent on the interactions, including electrostatic adsorption [35] and covalent bonds [36], between materials and solid supports. However, the disadvantages, including the long time required for surface modification and inhomogeneity of substrates, still need to be solved. The other fabrication methods, including deposition, in-situ growth, and immersion were seldom used, thus supporting the necessity of further development.

## 3. Categories of Solid SERS Substrates

Solid SERS substrates have drawn great attention for their features of solid characteristics, controllable morphology, and good stability compared traditional liquid substrates. Up to now, several solid SERS substrates, including membrane substrate, self-assembled substrate, chip-based substrate, magnetic substrate, and other solid substrates, have been fabricated for SERS analysis. Detailed information concerning representative solid SERS substrates, including categories, used materials, fabrication methods, analytical applications, and analytical performance, is listed in Table 1.

### 3.1. Membrane Substrate

The membrane substrate is one of the most common solid substrates for SERS analysis due to the easy preparation procedure, flexibility, satisfied enhanced performance, and good portability. Membrane substrates can be divided into paper membrane substrates, polymer membrane substrates, and non-support membrane substrates. The basic information, preparation procedure, and analytical performance of membrane substrates are introduced in detail.

### 3.1.1. Paper Membrane Substrates

The paper membrane substrate is a flexible solid SERS substrate based on the cellulose-based paper matrix with simple and convenient preparation process, including filtration [37], in-situ grown [38], printing/writing [39,40], self-assembly, and dropping/dipping [21,41]. Paper matrix shows promising spatial reticular structure for loading multifarious materials with high stability and capacity. To date, several materials have been used for the fabrication of paper membrane substrates, including noble metal [42], noble metals doped semiconductor composites [43], and noble metals embedded mesoporous material composite [44]. The dense distribution of “hot spots” originating from materials within limited space can significantly produce a good enhancement effect for SERS analysis. The noble metal is an ideal candidate due primarily to the simple preparation process and promising Raman signal enhancement. You’s group proposed a typical paper membrane substrate based on cellulose nanofiber-gold nanoparticles (CNF-AuNPs) composites via a simple filtration method (Figure 2a) [42]. The spatial distribution of AuNPs, including the number density and size ratio, can be precisely controlled, which can ensure the good enhancement signal due to the promising inter-particle plasmon coupling effects. The limit of detection (LOD) for rhodamine 6 G (R6G), thiram, and tricyclazole can reach 10.0 pmol/L, 1.0 pmol/L, and 10.0 pmol/L, respectively. This study provided a simple and novel strategy for improving SERS signals via controlling the spatial distribution of AuNPs on paper with nanoscale surface roughness via a simple and convenient preparation process. The noble metals doped semiconductor composite is an ideal SERS substrate due to the synergistic effect of localized surface plasmon resonance (LSPR) properties of noble metals and charge transfer of semiconductor. Our group [45] have developed a branched AuCu nanoalloy doped mesoporous graphitic carbon nitride hybrid hydrophobic membrane (mpg-C<sub>3</sub>N<sub>4</sub>/AuCu) for sensitive and selective analysis carcinogens including benzidine and zearalenone in food samples (Figure 2b). The high sensitivity was based on the design strategies of the anisotropic structure of AuCu, mesoporous semiconductor of mpg-C<sub>3</sub>N<sub>4</sub>, and hydrophobicity. The LOD for crystal violet (CV), benzidine and zearalenone were 1.0 ng/L, 0.14 µg/L and 0.03 µg/L, respectively. In addition, the stability and repeatability of mpg-C<sub>3</sub>N<sub>4</sub>/AuCu membrane substrate ensure the feasibility in practical SERS analysis. A black phosphorus-Au (BP-Au) filter paper membrane substrate was developed by Zhang’s group with low LOD of 1.0 nmol/L for CV molecule [43]. The paper membrane substrates based on noble metals doped semiconductor composite show superiorities in stability and SERS sensitivity compared to pure noble metals. The noble metals embedded mesoporous material composite has attracted increasing attentions due primarily to their significant preconcentrating and sieving effect. Recently, Au@ZIF-8 and UiO-66 (NH<sub>2</sub>)/AuNPs/Nylon-66 paper membrane substrates were respectively developed by Kang’s and Li’s group for trace analysis of contaminants in food samples [44,46]. The combination of mesoporous material with noble metals can selectively and effectively pre-concentrate targets in proximity to “hot spot” generated by noble metals according to the molecule size, suggesting the good SERS performance in sensitivity and selectivity. The paper membrane substrate shows great potential for largescale production due to the successful development of the multichannel filtering device and good serviceability for different types of materials.

**Table 1.** Summary of representative solid SERS substrates.

| Classification                  | Materials Used  | Fabrication Method                                | Stability/Reproducibility   | Targets                                  | LOD                                       | Samples              | Refs. |
|---------------------------------|---|---|---|--|---|----------------------|-------|
| Paper membrane substrates       | Ag/sandpaper/filter paper                             | Deposition  | RSD of 12.9% for 1600 points  | Ferritin antigen                         | 31.6 pg/L                                 | Water                | [47]  |
|                                 | mpg-C <sub>3</sub> N <sub>4</sub> /AuCu               | Filtration  | RSD of 14 consecutive days (4.8%) and 25 batches (2.7%)   | Benzidine                                | 0.14 µg/L                                 | Tea bag              | [45]  |
|                                 | GO-Au   | Immersing   | /   | Zearalenone                              | 0.03 µg/L                                 | Food sample          | [48]  |
|                                 | GO-GNS  | Filtration  | reproducibility of 3.6-8.9%   | Bilirubin                                | 7.0 µmol/L                                | Blood serum          | [21]  |
|                                 | Ti <sub>3</sub> C <sub>2</sub> T <sub>x</sub> /DNA/Ag | Filtration  | RSD of 4.1% for 42 days   | Bilirubin                                | 0.44 µmol/L                               | Blood serum          | [49]  |
|                                 |   |   |   | Nitrofurantoin                           | 12.0 µg/L                                 | Fish samples         |       |
|                                 |   |   |   | Ofloxacin                                | 35.0 µg/L                                 | Shrimp samples       |       |
| Polymer membrane substrates     | PDMS/Au   | Surface growth                                    | /   | <i>V. parahaemolyticus</i>               | 12 cfu/mL                                 | Oyster, salmon       | [50]  |
|                                 | Au NWs/PDMS   | In-situ grown                                     | mapping RSD values of 6.45% and 6.31% for PSA and AFP   | Prostatespecific antigen                 | 0.49 ng/L                                 | Serum                | [51]  |
|                                 | PVDF/Ag/MIP   | Mixed growth                                      | /   | α-fetoprotein                            | 0.72 ng/L                                 | Water                | [52]  |
|                                 | PMMA/GO/AuNSs   | Immersing<br>Spin coating                         | RSD less than 10.7% for SERS mapping; RSD of 4.7% for 600s irradiation  | <i>P. aeruginosa</i><br><i>S. aureus</i> | /   | Skin burn wound      | [53]  |
|                                 | PDMS/Ag   | Surface growth                                    | RSD of 5.6% for 6 random points   | 2,6-pyridinedicarboxylic acid            | 1.2 pmol/L                                | <i>B. subtilis</i>   | [54]  |
| Non-support membrane substrates | GNPs/g-C <sub>3</sub> N <sub>4</sub> /GO              | Filtration  | RSD of 14.1% 16 points within 4 batches   | R6G                                      | 0.05 pmol/L                               | Water                | [55]  |
|                                 | δ-MoN   | Filtration  | RSD less than 7.8% for 5000 measurement points  | 2,5-dichlorophenol<br>BPA                | 0.1 nmol/L                                | Water                | [56]  |
| Liquid self-assembly substrates | AuNRs   | Self-assembly                                     | RSD of 12.9% for 10 reuse   | R6G                                      | 1.0 nmol/L                                | Water                | [25]  |
|                                 | Au@Ag   | Self-assembly                                     | RSD of 10.5% for substrate-to-substrate   | Thiram                                   | 1.1 µg/L                                  | Water                | [27]  |
|                                 | AuNRs   | Solvent-assisted self-assembly                    | /   | Thiabendazole                            | 51.0 µg/L                                 | Water                | [57]  |
|                                 | Au core/Ag shell nanostar                             | Self-assembly                                     | RSD of 14.9% for 10 random points; 23 days for storage  | Pyocyanin                                | 1.0 pmol/L                                | <i>P. aeruginosa</i> | [57]  |
|                                 | AuNPs   | Self-assembly                                     | RSD of 2.7% for SERS mapping; RSD of 2.7% for 10 batches  | Dopamine                                 | 0.1 nmol/L                                | Water                | [58]  |
|                                 |   |   |   | <i>E. coli</i><br><i>S. aureus</i>       | 50 cfu/mL                                 | Serum                | [59]  |
| Solid self-assembly substrates  | MF/Ag   | Self-assembly;<br>In-situ grown                   | Good repeatability and reproducibility for different random sites, consecutive days, extreme temperature, and UV exposure | Dopamine<br>Lysozyme<br>Hemoglobin       | 2.69 fmol/L<br>62.0 pmol/L<br>6.83 pmol/L | Water                | [60]  |
|                                 | Au NB   | Template deposition;<br>Etching;<br>In-situ grown | /   | R6G                                      | 1.0 pmol/L                                | Water                | [61]  |
|                                 | Au/TiO <sub>2</sub>                                   | Template method;<br>Sputtering                    | /   | Exosomes                                 | /   | Plasma               | [62]  |
|                                 | Au/HCP-PS   | Spin coating;<br>Deposition                       | RSD less than 5% for reliability and reproducibility  | Tyrosine<br>Phenylalanine<br>Tryptophan  | /   | Tears                | [28]  |
|                                 | AuNPs   | Plasms etching<br>Sputtering                      | /   | alpha-fetoprotein- L3                    | 3.0 ng/L                                  | Water                | [29]  |
|                                 | AuNPs, AgNPs  | Etching<br>Deposition                             | RSD of 11.6% for 100 random points; RSD of 12% for 2000 spectra within 4 batches  | Pyocyanin                                | 6.25 µmol/L                               | Artificial sputum    | [63]  |

Table 1. Cont.

| Classification        | Materials Used                                       | Fabrication Method                     | Stability/Reproducibility   | Targets   | LOD                                     | Samples                                    | Refs. |
|-----------------------|--|--|---|---|---|--|-------|
| Chip-based substrate  | P4VP-g-GO/Ag   | Surface modification;<br>In-situ grown | /   | 4-aminothiophenol   | 0.1 pmol/L                              | Water                                      | [64]  |
|                       | Au@MIP   | Surface modification;<br>Spin coating  | RSD of 10.0–15.0% for SERS mapping                                    | Pyrene<br>Fluoranthene  | 1.0 nmol/L                              | Creek water;<br>Seawater                   | [31]  |
|                       | M-AuNP/PDMS/Au                                       | Surface modification                   | RSD of 3.8% for 10 random points                                      | Hematin   | 0.03 nmol/L                             | Human erythrocytes                         | [35]  |
|                       | SAuNPs@GO  | Surface modification                   | /   | Paclitaxel<br>Cyclophosphamide                                  | 15.0 nmol/L<br>5.0 nmol/L               | Blood serum                                | [36]  |
|                       | AuNPs  | Surface modification                   | /   | MCP-1<br>IL-10  | 0.1 ng/L                                | Human serum                                | [65]  |
|                       | AAO/Au NBPs  | Diffusion                              | RSD of 9.4% for 5 random points;<br>RSD of 9.6% for 5 batches         | Dopamine  | 6.5 nmol/L                              | Human serum                                | [66]  |
|                       | AuNPs/rGO/NFs  | Surface reduction<br>Surface growth    | /   | 6-mercaptopurine  | 0.5 nmol/L                              | Human plasma                               | [67]  |
| Magnetic substrates   | Fe <sub>3</sub> O <sub>4</sub> @Au                   | Surface modification                   | RSD of 7.6% for 30 random points                                      | Valosin-containing protein                                      | 25.0 ng/L                               | Human tissues                              | [68]  |
|                       | CoFe <sub>2</sub> O <sub>4</sub> @HNTs/AuNPs         | Surface modification                   | RSD less than 10% for reproductive determination                      | 4,4'-thioaniline<br>Nitrofurantoin                              | 26.0 µg/L<br>14.0 µg/L                  | Hair dyes<br>Fish feed;<br>Aquatic samples | [69]  |
|                       | Fe <sub>2</sub> O <sub>3</sub> @AgNPs                | Thermal decomposition                  | /   | <i>P. gingivalis</i><br><i>A. actinomycetemcomitans</i>         | /                                       | Human saliva                               | [70]  |
|                       | Fe <sub>3</sub> O <sub>4</sub> @SiO <sub>2</sub> @Au | Surface modification                   | RSD less than 11.0% for reproductive determination                    | <i>S. aureus</i><br><i>A. baumannii</i><br><i>K. pneumoniae</i> | 14.1 fmol/L<br>9.7 fmol/L<br>8.1 fmol/L | MDR bacteria-infected mice                 | [71]  |
|                       | Fe <sub>3</sub> O <sub>4</sub> @Ag                   | Surface modification                   | RSD of 3.7% and 5.8% for 30 consecutive test in water and human serum | miRNA-122<br>miRNA-223<br>miRNA-21                              | 349 amol/L<br>374 amol/L<br>311 amol/L  | Human serum                                | [72]  |
| Other solid substrate | hBN/AgNWs/sponge                                     | Mixed modification                     | RSD of 8.0% for 30 random points                                      | RhB   | 10.0 nmol/L                             | Water                                      | [73]  |
|                       | Au-G-AgNs  | Surface modification                   | RSD of 9.2% for 30 random points                                      | MG  | 0.1 nmol/L                              | Water                                      | [74]  |
|                       | Ag-cotton  | Surface modification<br>Tabletting     | RSD of 7.5% for 10 random points                                      | <i>E. coli</i>  | /                                       | Urine                                      | [75]  |

### 3.1.2. Polymer Membrane Substrate

The polymer membrane substrate is a typical flexible and transparent membrane substrate compared to conventional rigid and nontransparent substrates, providing a direct method for the analysis of molecules on irregular and nonplanar surfaces by simple covering [76]. Commonly used polymers are polydimethylsiloxane (PDMS) and poly(vinylidene fluoride) (PVDF) according to their promising thermodynamic properties, low cost, and ease of preparation [35,52]. In general, surface modification and assembly methods have been adopted for the fabrication of polymer membrane substrates [77,78]. Li et al. developed Ag nanocubes@PDMS film (Ag NCs@PDMS) via the assembly method for SERS analysis with high performance [79]. The dense Ag NCs arrays were formed at the cyclohexane/water interface via a three-phase system (water, ethanol, and cyclohexane), followed by the replacement of cyclohexane by PDMS mixture to form a flexible Ag NCs@PDMS film on the top (Figure 2c). The uniform and dense distribution of Ag NCs on PDMS matrix ensure the promising SERS signal enhancement, as well as good stability and flexibility for SERS analysis. The LOD for methylene blue (MB) and R6G can reach 0.1 and 1.0  $\mu\text{mol/L}$ . A PDMS based membrane substrate modified with forest of Ag/Au nanowires (Ag/Au NWs/PDMS) was developed by Jiang's group via surface modification for multiphase SERS analysis [80]. The separated PDMS film was first prepared by simple spin coating. Then, Au nanowires were in-situ grown on the PDMS film, followed by magnetron sputtering of Ag (Figure 2d). The integration of Au/Ag NWs and PDMS film provides a simple and novel strategy for the fabrication of a polymer membrane substrate with high SERS sensitivity (LOD = 1.0  $\mu\text{mol/L}$  for 2-naphthalenethiol). In addition, some metal-semiconductor composites were immobilized on polymer membrane-based substrate for improving the SERS sensitivity and maintaining the stability, such as PDMS/TiO<sub>2</sub>/Ag [81], AgNW@rGO-PEI/PVDF-HFP [82], and Cu@rGO-PEI@AgNWs [83] membrane substrates. The polymer membrane substrate shows unique superiorities in accurate contact with samples, high SERS sensitivity, and easiness in tailoring. However, the polymer membrane substrate also meets limitations in short storage time and single enhanced material.

### 3.1.3. Non-Support Membrane Substrate

The non-support membrane substrate is a new kind membrane substrate without support, which was usually fabricated by a filtration process, with subsequent peeling from the supporter. The good membrane-forming property is mainly dependent on the mechanical and two dimensional (2D) properties of as-fabricated materials. Graphene (GO) based composite is promising in the fabrication of non-support membrane substrates on the basis of its good membrane-forming property and enhancement effect [84]. Ding's group developed a non-support membrane based on multilayer graphene and AgNPs by cross-section strategy, maximizing the plasmonic coupling of AgNPs [24] (Figure 3a). The LOD for R6G can reach 0.5 pmol/L with long-term stability. The A multifunctional non-support membrane was prepared by intercalating gold nanoparticles (GNPs) and graphitic carbon nitride (g-C<sub>3</sub>N<sub>4</sub>) into graphene oxide nanosheets (GNPs/g-C<sub>3</sub>N<sub>4</sub>/GO) for SERS analysis of 4-chlorophenol at nanomolar level [55]. The sheet-like g-C<sub>3</sub>N<sub>4</sub> and GO provide membrane-forming property, a loading site for GNPs, and CM effect all-in-one. Furthermore, Xi's group developed several non-support membrane substrates based on pure transition metal oxides/nitrides, including N-TiO,  $\gamma$ -Mo<sub>2</sub>N, and  $\delta$ -MoN, for high SERS analysis with good performance [23,56,85]. The high requirement for the fabrication of non-support membrane substrates indicates the great space for exploring new matrix material with good membrane-forming property. The non-support membrane substrates also show promising potential for commercialization in practical applications by virtue of their simple fabrication procedure and strong toughness.

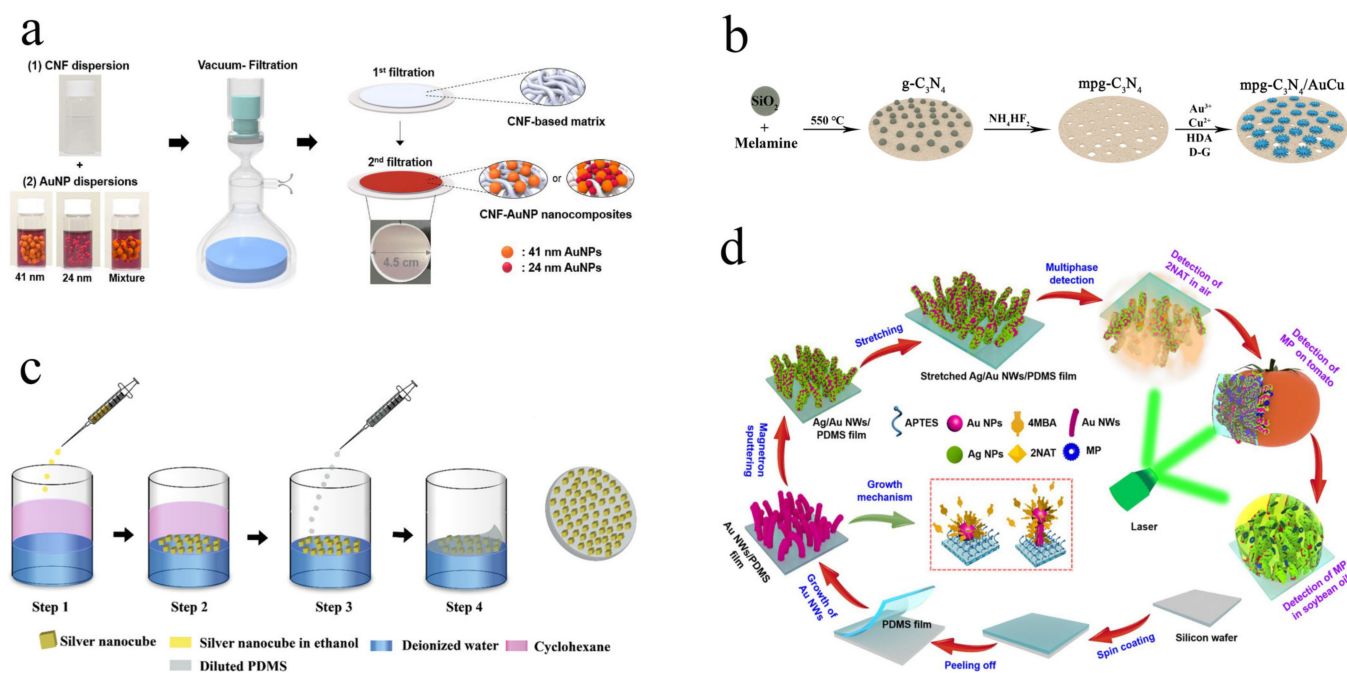


**Figure 2.** Schematic fabrication of CNF-AuNP membrane substrate (a). © 2022 Elsevier B.V. Adapted with permission from [42]. Schematic illustration of preparation principle of mpg-C<sub>3</sub>N<sub>4</sub>/AuCu membrane (b). © 2022 Elsevier B.V. Adapted with permission from [45]. Schematic illustration of fabrication process of Ag NCs@PDMS substrate (c). © 2022 American Chemical Society. Adapted with permission from [79]. Schematic preparation of Ag/Au NWs/PDMS film and its application for on-site detection of pesticides (d). © 2022 Elsevier B.V. Adapted with permission from [80].

### 3.2. Self-Assembled Substrate

Self-assembled substrates have widely adopted for SERS analysis according to their controllable morphology and dense distributions of “hot spots”. Liquid self-assembly substrates and solid self-assembly substrates are the main two important forms, usually fabricated by liquid metallic colloids and solid template array, respectively. Compared to membrane substrates, self-assembled substrates show unique advantages, including precise control of morphology, lateral spacing, and macroscale homogeneity [57]. The precise control of noble metals at nanoscale ensures the significant and stable SERS signals, exhibiting great potential for SERS analysis.

#### 3.2.1. Liquid Self-Assembly Substrate

Liquid self-assembly substrate with solid form mainly refers to the self-assembled metallic colloids transferred to the surface of the support film. The three-phase system (water-ethanol-cyclohexane/hexane/chloroform) is commonly applied for the fabrication of self-assembled metallic colloids interface under the guidance of drying-mediated self-assembly mechanism [27,86]. The metallic colloids can be driven to a limited area without a decrease in number, making significant and stable enhanced Raman signals due to the dense and uniform distribution of “hot spots”. Sun’s group fabricated an interfacial self-assembly gold nanorods (Au NRs) array for the simultaneous screening of thiram and thiabendazole (TBZ) in fruits with high sensitivity and reproducibility (Figure 3b) [87]. The LOD for thiram and TBZ are 36.0 pmol/L and 0.95 nmol/L with relative standard deviation (RSD) less than 10%. In addition, several self-assembly strategies have been adopted in the precise control of size, lateral spacing, morphology, and uniformity, such as organic solvent assist [25,57], convective self-assembly [26], electrostatic repulsion combined with depletion attraction [88], and ligand exchange [89], etc. The above self-assembly strategies show identical superiority in the self-assembly of anisotropic noble metals, which can

significantly improve the SERS sensitivity on the basis of their denser “hot spot” and tuned surface plasmon resonance (SPRs) properties [90,91]. However, the instability of noble metals over time limits their practical applications in SERS analysis, needing to be solved or improved urgently.

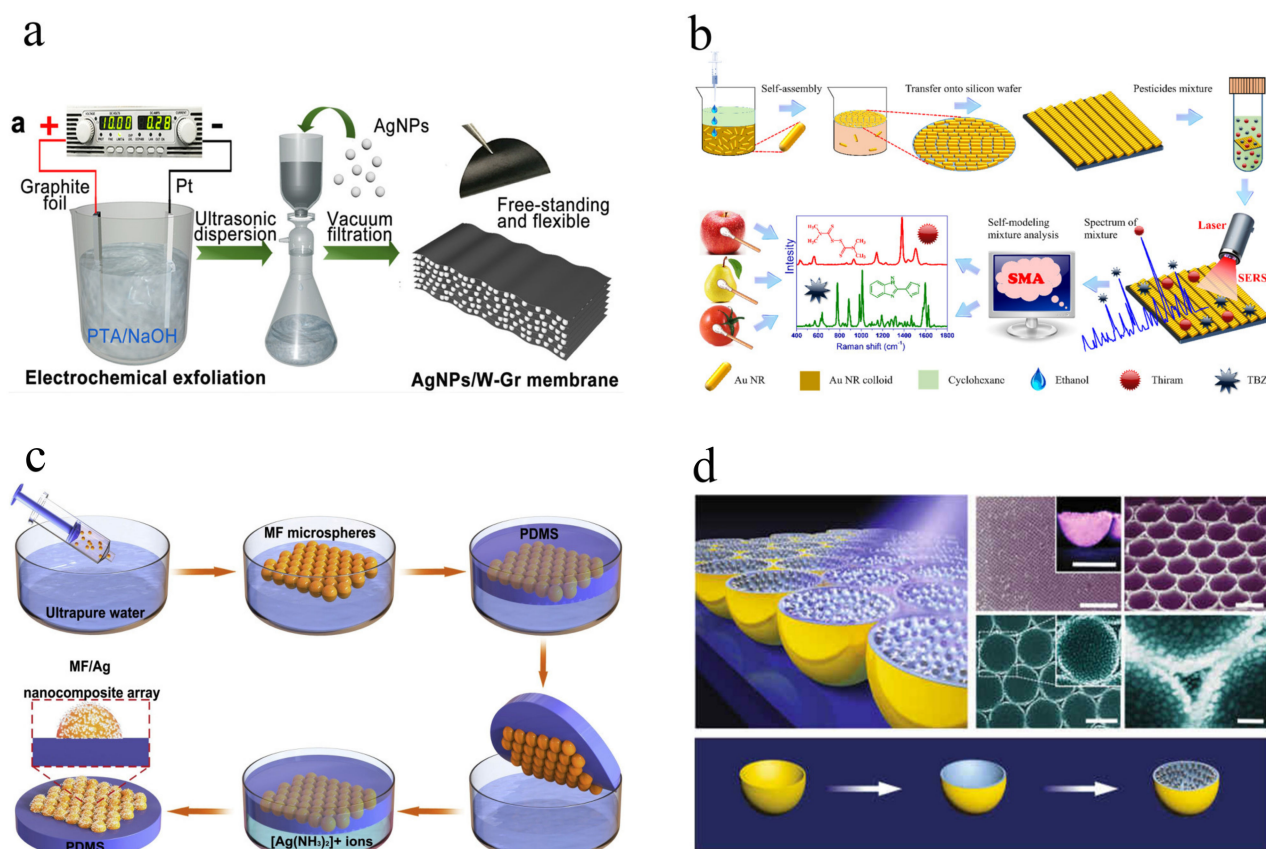


**Figure 3.** Schematic of the fabrication process of the AgNPs/W-Gr membrane (a). © 2022 Elsevier B.V. Adapted with permission from [24]. Schematic preparation of self-assembly gold nanorods (Au NRs) array and detection of pesticides on fruit surface (b). © 2022 Elsevier B.V. Adapted with permission from [87]. Schematic preparation diagram of hierarchical MF/Ag array substrate (c). © 2022 Elsevier B.V. Adapted with permission from [60]. Schematic illustration of preparation of NP-on-WS hierarchical substrate (d). © The Author(s) 2018. Adapted with permission from [61].

### 3.2.2. Solid Self-Assembly Substrate

Solid self-assembly substrates are composed of periodic solid array supports and noble metals, which have similar advantages to the liquid self-assembly substrate in satisfied and stable SERS signals thanks to the solid array supports and uniform distribution of “hot spots”. Furthermore, some chemically stable supports also provide a good protective effect for noble metals, which can significantly extend storage time and expand the scope of SERS analysis. In general, periodic template (PS, SiO<sub>2</sub>, and MF) mediated arrays are commonly used supports for the fabrication of solid self-assembly substrates [60,92,93]. The monolayer periodic templates are first assembled at the gas–liquid interface and then transferred to the solid film. After that, the noble metals can be deposited on the surface of monolayer periodic templates via several methods, including magnetron sputtering [30], in-situ grown [60], surface modification [93], and deposition [28]. Deng et al. developed a hierarchical superhydrophobic melamine-formaldehyde/Ag (MF/Ag) array for the SERS analysis of biomolecules with good sensitivity and reproducibility (Figure 3c) [60]. The LOD of MF/Ag array for dopamine, lysozyme, and hemoglobin is 2.69 fmol/L, 62.0 pmol/L and 6.83 pmol/L, respectively. The good repeatability of the MF/Ag array was confirmed in

several situations, including random sites, consecutive days, extreme temperature, and UV exposure. In addition, the periodic templates can also be designed and fabricated with different morphology, size, and spacing for more sensitive and stable SERS signals [29,92,94]. Apart from the direct modification of noble metal on templates, the solid templates can be removed to obtain vacancy with controllable morphology before noble metal modification [95–98]. A solid self-assembly substrate based on warped spaces to manipulate hotspots was developed by Chen's group (Figure 3d) [61]. The Au nanobowl (Au NB) was firstly obtained by the template metal deposition method combined with etching method, followed by e-beam evaporation of thin SiO<sub>2</sub> film. Finally, nanoparticles on a warped substrate (NP-on-WS) can be achieved by the gas-phase deposition method with AgNPs. The warped spaces of NP-on-WS substrate can significantly enhance broadband electromagnetic energy within large spectral regions, inducing promising SERS signals for R6G. In addition, some materials, including copper oxide (CuO) [99], graphene [100], and functional self-assembled monolayer [101], were applied to the fabrication of solid self-assembly substrates to improve the sensitivity, stability, and selectivity of the SERS method. In terms of practical SERS analysis, solid self-assembly substrates show better potential for commercialization compared to liquid self-assembly substrates on account of their stability, several available materials, and ease of modification. However, the fabrication method for solid self-assembly substrates needs to be simplified to meet the requirements for practical application.

### 3.3. Chip Substrate

The chip-based substrate is an important supplement to the solid self-assembly substrate, especially during the preparation process. The fabrication of a solid self-assembly substrate is mainly based on periodic templates combined with the self-assembly strategy. However, chip-based substrates show more strategies, including in-situ grown [102], spin coating [36], electrochemical deposition [103], surface modification [104], and magnetron sputtering [33], etc. Thus, the structure of chip-based substrates can be designed and fabricated to meet the requirements of SERS analysis in terms of sensitivity, selectivity, and stability. A novel 3D Ag mesoflowers (Ag MFs) modified poly(4-vinylpyridine) brush-grafted-graphene oxide (P4VP-g-GO) films was developed by Chen's group (Figure 4a) [64]. The obtained Ag nanoporous mesoflowers show large specific surface area and highly rough surface, resulting in ultra-sensitivity for the SERS analysis of 4-aminothiophenol with LOD of 0.1 pmol/L. Furthermore, the chip-based substrate with high selectivity for SERS analysis can be achieved via combination with the molecular imprinting technique (MIP) [105]. The MIP based method shows advantages in selectivity, versatility, and predictability, suggesting good feasibility for specific recognition in SERS analysis. Pastoriza-Santos's group [31] has reported a reliable and selective molecularly imprinted chip-based SERS substrate (Au@MIP) for the highly selective analysis of polycyclic aromatic hydrocarbons (PAHs), including pyrene and fluoranthene (Figure 4b). The AuNPs were first deposited on the glass by the layer-by-layer method and then coated with thin MIP film for the fabrication of an Au@MIP chip substrate. The good SERS activity and selectivity of the developed method based on the Au@MIP chip substrate can be obtained through a short distance between SERS active regions and specific sites of molecules. Moreover, some chip-based substrates with satisfactory stability have been designed and fabricated. Yim's group [106] developed a two-dimensional (2D) monolayer/Ag nanoparticle (AgNP) substrate with long-term oxidative stability. The AgNPs were assembled on the (3-aminopropyl) trimethoxysilane (APTMS) modified Si substrate, then covered by monolayer graphene or hexagonal boron nitride (h-BN). The hybrid platform of h-BN/AgNPs exhibited long-term SERS stability over 80 days, which can be attributed to the high chemical stability of monolayer h-BN. In addition, the h-BN/AgNPs substrate showed better stability compared to the graphene/AgNPs based substrate due to their different electrical and chemical properties. The chip-based substrates provide an effective

way of selecting an appropriate preparation strategy according to requirement of practical SERS analysis, which is more likely to be commercialized.

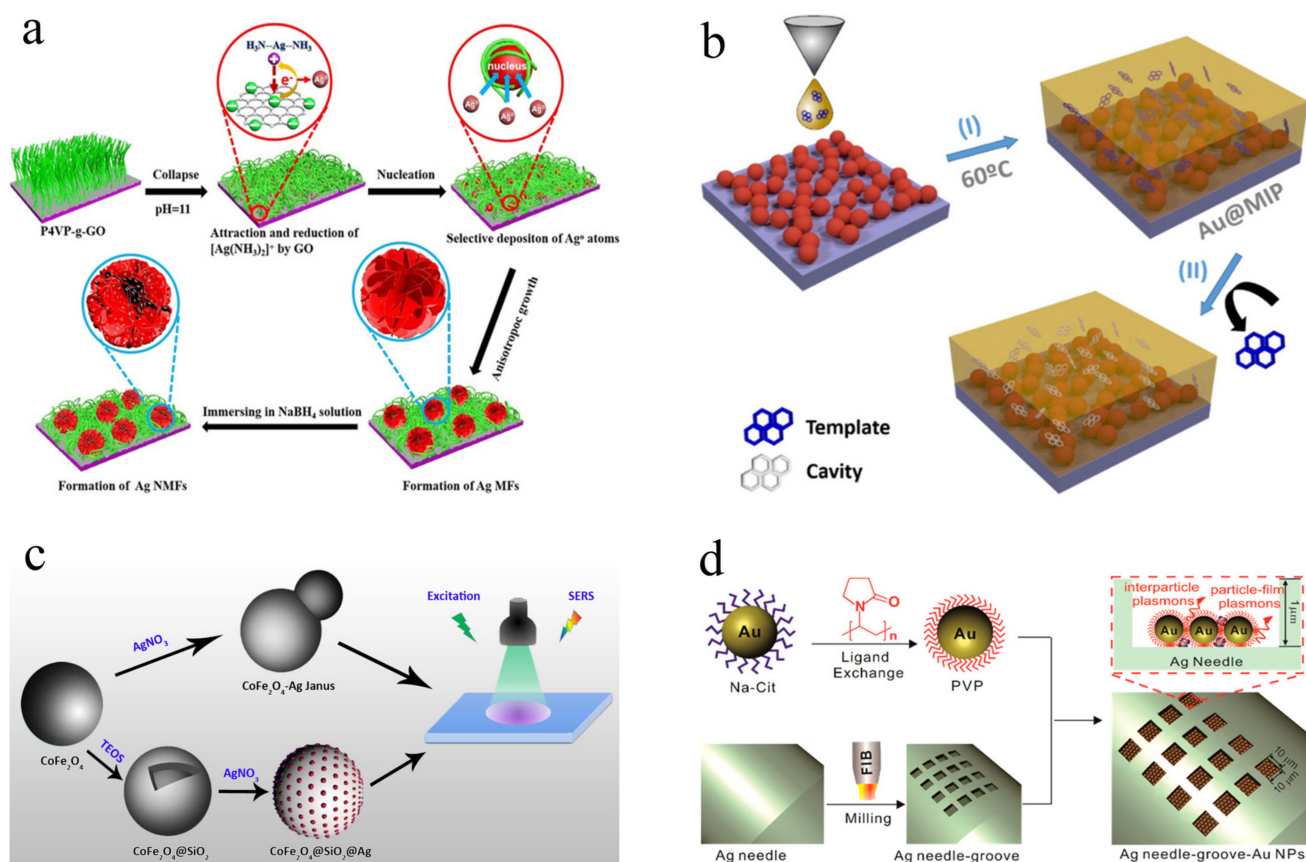


**Figure 4.** Schematic procedure for fabricating of 3D Ag MFs and Ag NMFs on P4VP-g-GO films (a). © 2022 Wiley-VCH Verlag GmbH & Co. KGaA. Adapted with permission from [64]. Schematic illustration of preparation of Au@MIP film (b). © 2022 American Chemical Society. Adapted with permission from [31]. Schematic synthesis of CoFe<sub>2</sub>O<sub>4</sub>/Ag substrate (c). © 2022 American Chemical Society. Adapted with permission from [107]. Schematic synthesis of Au-G-AgNs (d). © 2022 American Chemical Society. Adapted with permission from [74].

### 3.4. Magnetic Substrate

Magnetic substrates represent a class of solid substrate with unique features of magnetic properties and SERS activity, which can realize sample pretreatment and in-situ SERS analysis all-in-one. In addition, the promising magnetic separation properties of magnetic substrate endows them with solid-like characteristic for SERS analysis. In general, the magnetic solid substrate shows the typical structure of a plasmonic substrate over a magnetic core (P-o-M) [70]. Wei et al. have reported two magnetic solid SERS substrates with P-o-M structure, including CoFe<sub>2</sub>O<sub>4</sub>@SiO<sub>2</sub>@Ag and CoFe<sub>2</sub>O<sub>4</sub>-Ag Janus (Figure 4c), which show good SERS activity due to the strong SPR effect of AgNPs and special micro-nano structure [107]. Furthermore, the developed two magnetic solid substrates also exhibit a stable SERS signal at about 90% after five repeated uses. In addition, the SERS performance of magnetic solid substrates can also be improved by several strategies. Two ternary magnetic MOF-based substrates of Fe<sub>3</sub>O<sub>4</sub>@Au@MIL-100 (Fe) [108] and CoFe<sub>2</sub>O<sub>4</sub>@HNTs/AuNPs [69] with high SERS activity have been developed, benefitting from the good adsorption property of MOFs and HNTs, respectively. A Fe<sub>3</sub>O<sub>4</sub>@TiO<sub>2</sub>@Ag [51] magnetic substrate has been fabricated to improve SERS activity by using the synergistic effect of semiconductor characteristics of TiO<sub>2</sub> and SPR properties of Ag. Several selective reagents have been used to improve the selectivity of the SERS method based on magnetic solid

substrate, such as aptamer [71], antibody [109], cyclodextrin [68], and molecular imprinted polymer [110], etc. It should be noted that the stability and repeatability of SERS signal induced by magnetic solid substrates still meet limitations in terms of oxidation of the magnetic core and uneven distribution of plasmonic nanoparticles. Thus, the development of the SERS method based on magnetic solid substrate with promising stability as well as good sensitivity should be focused on in the future.

### 3.5. Other Solid Substrate

Apart from above four types of solid SERS substrates, there are some other solid SERS substrates that have been developed without specific classifications. Jun et al. [111] developed a hydrophobic sponge substrate via the deposition of silver nanowires coated h-BN composites on melamine-sponge (h-BN/AgNWs/sponge). The hydrophobic sponge substrate shows two important roles in the separation of organic pollutants via hydrophobic treatment and  $\pi$ - $\pi$  interactions, as well as in-situ monitoring the absorption process of organic pollutants by the SERS method. An Au nanoparticles-decorated silver needle (Au-AgNs) was prepared by Zhou's group for the ultrasensitive SERS analysis of malachite green (MG) in aquaculture products with low LOD of 0.1 nmol/L (Figure 4d) [74]. The surfaces of AgNs were milled to a groove array ( $10 \times 10 \mu\text{m}$ ) by focused ion-beam-scanning electron microscopy instrument equipped with a gallium-ion beam, followed by surface encapsulation of polyvinylpyrrolidone (PVP) modified AuNPs. The groove arrays not only provide reproducible SERS signals, but also avoid erasing AuNPs during insertion process. In addition, AgNPs decorated eggshell membrane [112] and adhesive tape-based substrate [113] were also reported for SERS analysis with high performance. These solid SERS substrates open a new vision for the fabrication of SERS substrate, as well as provide more choices for practical SERS analysis.

## 4. The Applications of Solid SERS Substrates

In view of the unique advantages of solid SERS substrates, several practical applications in fields of bio-analysis, food safety analysis, environment analysis, and biomedicine/public safety analysis have been reported. Here, we briefly introduce the specific examples of solid SERS substrates in fields mentioned above.

### 4.1. Bio-Analysis

With the rapid development of society and economy, the requirements for human health becoming higher and higher. Thus, development of high-quality solid SERS substrate for bio-analysis has attracted increasing attention [54,114]. The solid SERS substrates have been used for pathogen analysis with single molecule sensitivity and promising stability. Guo et al. developed an adhesive tape based solid platform for the analysis of wound infectious pathogens with the special advantage of three-in-one, namely rapid sampling, photocontrolled release, and SERS detection [53]. The dense distributions of gold nanostars were sandwiched between two layers of monolayer graphene modified by selective reagent (*o*-nitrobenzyl derivative) for wound infectious pathogens (Figure 5a). Hence, the sensitive, stable, and selective SERS analysis of *Pseudomonas aeruginosa* (*P. aeruginosa*) and *Staphylococcus aureus* (*S. aureus*) could be achieved. The developed "three-in-one" platform opened up new horizons in applications of point-of-care (POC) by the SERS method with satisfactory analytical performance. Tian et al. [59] reported self-assembled plasmonic nanoarrays for the simultaneous and sensitive reproducible analysis of various bacteria with concentrations in the range of 50–2000 CFU/mL. The self-assembled GNPs show dense and uniform "hot spots", making stable and reproducible SERS signals for the analysis of eight bacteria. Moreover, Zhao et al. [115] fabricated a magnetic aptamer-conjugated  $\text{Fe}_3\text{O}_4@Au$  ( $\text{Fe}_3\text{O}_4@Au\text{-Apt}$ ) substrate for the selective and sensitive SERS analysis of *S. aureus*. The LOD for *S. aureus* can reach 25 CFU/mL with cell capture efficiency (CCE) of 68%. This multifunctional magnetic solid substrate integrated

the advantages of specific recognition, sensitive SERS detection, and photothermal therapy (PTT) of *S. aureus*.

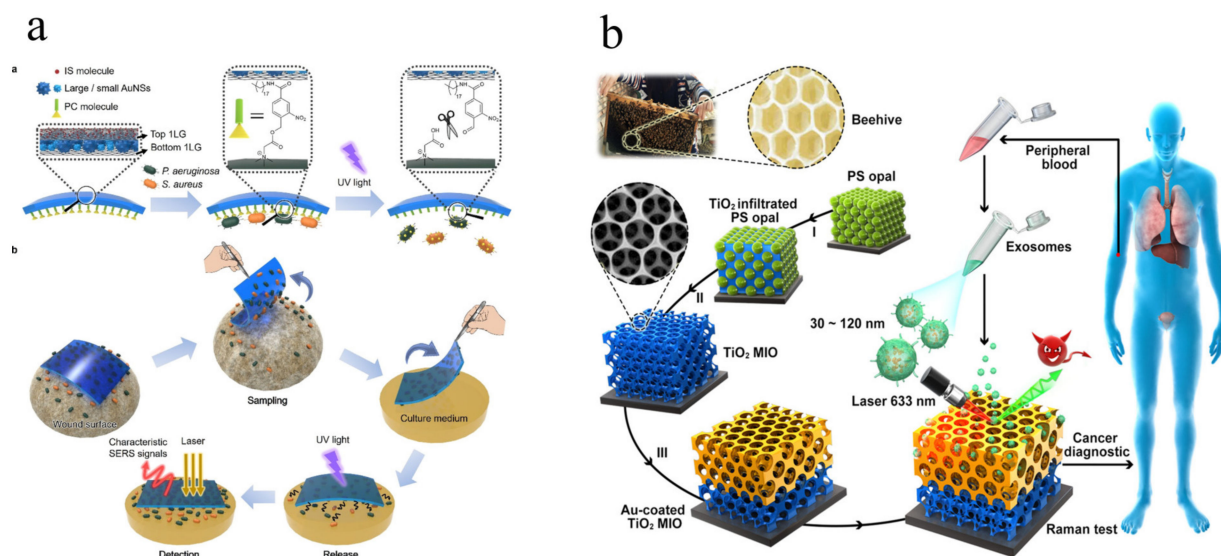


**Figure 5.** Schematic fabrication of adhesive tape based solid platform and its applications in rapid sampling, photocontrolled release, and on-site SERS detection (a). © 2022 American Chemical Society. Adapted with permission from [53]. Schematic preparation of Au-coated TiO<sub>2</sub> MIO and its detection process (b). © 2022 American Chemical Society. Adapted with permission from [62].

Apart from pathogens, several biomarkers of disease have been accurately determined with the SERS method by solid SERS substrate. Dong et al. [62] developed a beehive-inspired macroporous solid SERS substrate for the label-free analysis of the protein phosphorylation status of exosomes (biomarker of cancer) (Figure 5b). The multiple layers of PS opal templates were spin-coated on the Si wafer, followed by TiO<sub>2</sub> precursor infiltration into the interstitials. After annealing, PS templates can be removed, and the TiO<sub>2</sub> macroporous inverse opal (MIO) structure can be obtained. Finally, the MIO structure TiO<sub>2</sub> framework was covered by thin Au film to form a beehive-inspired macroporous solid SERS substrate. The exosomes from plasma can be effectively captured and analyzed due to the macroporous structure, which was applied to identify cancer patients successfully by recording the SERS intensity of phosphoproteins (P-O bond) at 1087 cm<sup>-1</sup>. Kim et al. [28] developed gold-decorated hexagonal-close-packed polystyrene (Au/HCP-PS) chip-based substrate for the noninvasive and real-time analysis of biomarkers of asymptomatic breast cancer in human tears. The fabricated Au/HCP-PS arrays used for SERS analysis show ultra-sensitivity at femtomole-scale and good reproducibility (with RSD less than 5%) thanks to the periodic distribution of template and uniform distribution of AuNPs, respectively. A graphene oxide-gold nanostar (GO-GNS) hybrid membrane substrate was fabricated by Pan's group for the label-free and rapid analysis of serum bilirubin (biomarker of jaundice) [21]. The LOD of the developed method based on GO-GNS hybrid membrane substrate for serum bilirubin can reach 0.436 μmol/L, attributed to the integration of enrichment effect and chemical enhancement of GO, and the dense "hot spot" of GNS. Li's group developed a polytetrafluoroethylene (PTFE)-based membrane substrate for the sensitive detection of atherosclerosis-related biomarkers (cytokines), including IL-10 and MCP-1 [65]. A sandwich-like membrane substrate was fabricated by antibody modified AuNPs deposited nanoporous networking PTFE membrane for SERS analysis with high sensitivity (0.1 pg/mL for IL-10 and MCP-1) and specificity. The solid SERS substrates provide great potential in the label-free, rapid, sensitive, and on-site analysis of biomarkers of diseases, which will play a more important role in clinical diagnosis and treatment.

In addition, solid SERS substrates have also been applied to the analysis of some biomolecules with promising performance. Cai et al. [35] developed a flexible polymer membrane substrate of multibranching AuNPs embedded in polydimethylsiloxane (M-AuNPs-PDMS) for the accurate and direct analysis of hematin in erythrocytes without a separation process. The LOD for hematin can reach 0.03 nmol/L, which can be attributed to the synergistic effect of close contact between M-AuNPs and hematin, and plasmon coupling between the M-AuNPs and the Au film. A chip-based substrate of GO-supported L-cysteine-functionalized starlike AuNPs (L-cysteine SAuNPs@GO) was reported by Panikar et al. [36] for the analysis of paclitaxel and cyclophosphamide in serum samples. The space between the SAuNPs can be precisely controlled to 2.28 nm, confirming great SERS signals. In addition, L-cysteines play an important role in the brush layer to avoid the blocking of “hot spot” and fouling by proteins in serum. The LOD for paclitaxel and cyclophosphamide are 15.0  $\mu\text{mol/L}$  and 5.0  $\mu\text{mol/L}$  with high reproducibility. The SERS method based on solid substrates will play a vital role in the analysis of biomolecules with unique features of label-free, on-site, sensitivity, and stability.

#### 4.2. Food Safety Analysis

In recent years, food safety issues have attracted increasing attention due to their close relationship with public health. Several food contaminants, including mycotoxins [116], pesticides [27], and food additives [117], show features of low concentration and high toxicity, demanding an appropriate analytical method to meet the requirements of trace analysis. The solid substrate is a promising candidate for SERS application with dense “hot spot”, high stability, controllable morphology, and convenient portability. Here, we briefly introduce the specific analysis applications for food contaminants based on solid SERS substrate.

Mycotoxins are class of important biotoxins in foods with widespread distribution, high toxicity, and thermal stability, indicating great potential threat to human health via several routes [118,119]. Considering the unique features of SERS method, solid SERS substrates can be used for analysis of mycotoxins with high analytical performance. Li et al. [33] fabricated cauliflower-inspired chip-based SERS substrate for simultaneous and label-free analysis of multiple mycotoxins in maize including aflatoxin B1 (AFB<sub>1</sub>), deoxynivalenol (DON), and zearalenone (ZEN) (Figure 6a). The LOD for 4-mercaptobenzoic acid (4-MBA), AFB<sub>1</sub>, DON, and ZEN are 0.15 pg/mL, 1.8, 47.7, and 24.8 ng/mL, respectively. Furthermore, the RSD of as-fabricated chip substrate for random 40 sites detection of 4-MBA was 4.57%, exhibiting excellent repeatability for SERS analysis. Shao et al. [120] developed a magnetic solid substrate based on Au(core)@Au-Ag(shell) modified Fe<sub>3</sub>O<sub>4</sub> (Au@AuAg-MNP) for highly sensitive and selective detection of ochratoxin A (OTA) in red wine. The magnetic solid features combined with aptamer endowed with promising repeatability and selectivity by SERS method. Rostami et al. [121] fabricated Ag-capped silicon nanopillar array combined with supported liquid membrane (SLM) extraction for label-free and sensitive analysis of OTA in wine samples. The detection system achieves integrations of enrichment, high throughput and on-site detection, which has successfully applied to trace SERS analysis of OTA in wine samples with high sensitivity (LOD = 113  $\mu\text{g/L}$ ). Considering the wide distribution and high toxicity of mycotoxins, solid SERS substrates shows great potentials in on-site, high throughput, sensitive and stable detection of mycotoxins.

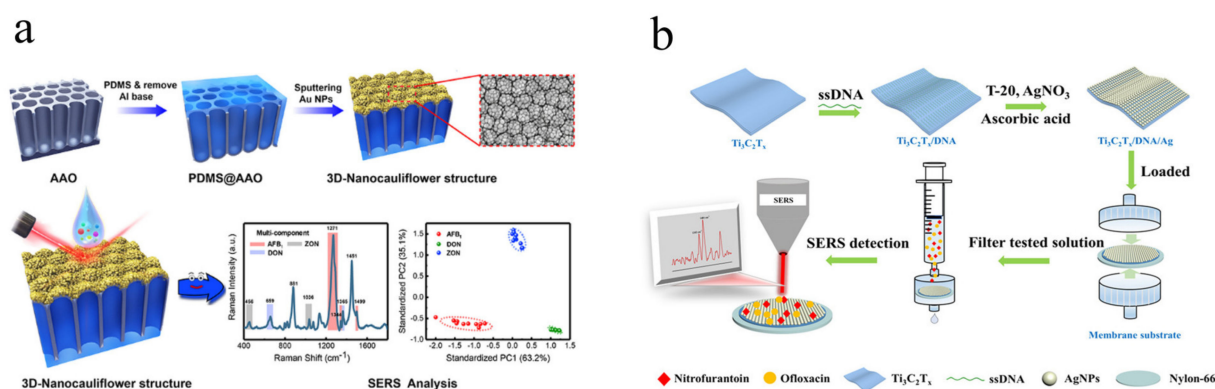


**Figure 6.** Schematic fabrication of cauliflower-inspired chip-based SERS substrate for simultaneous label-free analysis of multiple mycotoxins (a). © 2022 American Chemical Society. Adapted with permission from [33]. Schematic preparation process of the  $\text{Ti}_3\text{C}_2\text{T}_x/\text{DNA}/\text{Ag}$  membrane substrate and its application of simultaneous and accurate quantification of multiple antibiotics (b). © 2022 American Chemical Society. Adapted with permission from [49].

Pesticides are major pollutant sources of food, especially in vegetables and fruits, needing a stable SERS substrate for rapid, sensitive and trace analysis. Ma et al. [77] fabricated a flexible and transparent gold nanobush-PDMS hybrid membrane substrate (AuNB-PDMS) for analysis of TBZ in cherry samples. The grown AuNB on PDMS provides uniform and dense distribution of “hot spot”, indicating the sensitive and stable SERS signals. The flexible and transparent membrane substrate can realize in-situ and swabbing detection of TBZ with LOD of 0.64 ng/mL, which is suitable in on-site monitoring pollution status of TBZ. Wang et al. [122] developed a superhydrophobic membrane substrate for trace analysis of nitenpyram (NIT) based on silver dendrite-decorated filter paper. The superhydrophobic treatment can avoid randomly spreading of analytes, ensuring efficient sample collection. Additionally, anisotropic structure of fern-like silver dendrites provide uniform and strong electromagnetic field to enhance SERS signals and the LOD of NIT can reach 1.0 nmol/L. Xie et al. [123] fabricated a flexible membrane substrate with multiple “hot spots” based on three-dimensional (3D) AuNPs modified PDMS (Au@PDMS) for highly sensitive SERS analysis of pesticide residues. The membrane substrate shows typical features of flexibility and portability, exhibiting great potential in rapid and on-site detection of thiram on the nonplanar surface of vegetables and fruits. The flexible membrane substrates are more suitable for on-site, rapid and sensitive SERS analysis of pesticides according to their promising portability and deformability.

Food additives are important class of additives added to foods in order to significantly improve the quality or shelf life of food. However, several food safety issues caused by abuse or illegal addition of food additives remind that development of effective analytical method for monitoring food additives in food is still urgently required. Li’s group reported a  $\text{Ti}_3\text{C}_2\text{T}_x/\text{DNA}/\text{Ag}$  membrane substrate for simultaneous analysis of multiple antibiotics including nitrofurantoin (NFT) and ofloxacin (OFX) in aquatic samples (Figure 6b) [49]. The good sensitivity of SERS method based on  $\text{Ti}_3\text{C}_2\text{T}_x/\text{DNA}/\text{Ag}$  membrane substrate can be attributed to the excellent electromagnetic enhancement (EM) combined with chemical enhancement (CM). In addition, the promising uniformity, reproducibility, stability of as-fabricated membrane substrate was verified by several characterizations. The  $\text{Ti}_3\text{C}_2\text{T}_x/\text{DNA}/\text{Ag}$  membrane substrate integrated a series of features of multitarget separation, enrichment, and in-situ detection. Luo et al. [124] developed flexible Ag nanowires embedded PDMS (Ag NWs@PDMS) membrane substrate for detection of MG residue in food samples. The as-fabricated Ag NWs@PDMS film shows great durability and recyclability in several situations including 20 times stretchability,  $\text{HNO}_3$  corrosion, ultrasonication and broad temperature in range of  $-20$ – $80$  °C. The sensitivity of developed SERS method based on Ag NWs@PDMS film was proved by quantitative detection MG in

juices with LOD of 10.0 nmol/L. Kumar et al. [40] developed paper-based substrate by step-by-step printing method for sensitive and reproducible SERS analysis of non-permitted colourants including Metanil Yellow (MY) and MG. The Ag nanowires were in-situ grown on the printed area with high density, indicating the high sensitivity and reproducibility for SERS detection. Nie et al. [97] fabricated bowl-like pore array belong to solid self-assembly substrate for SERS detection of melamine in milk powder. The periodic hollow Au/Ag alloy array exhibits great SERS activity for melamine with LOD of 1.0  $\mu\text{mol/L}$ , which meets the requirement of trace analysis of melamine in milk powder. The solid SERS substrates will play an important role in monitoring the abuse or illegal addition for food additives.

#### 4.3. Environment Analysis

With the rapid development of economy and industry, environmental pollutants become more and more serious in diversities, wide sources, and high toxicity. Thus, developing advanced solid substrate for rapid, on-site, and sensitive SERS analysis of environmental pollutants is a good choice. Organic dyes are class of widespread pollutants, which have several sources including soil, water source, plants, and aquatic product, etc. Ji et al. [125] designed a chip-based substrate with sandwich structure of Ag/Cu<sub>2</sub>O/ITO by electrochemical deposition combined with in-situ reduction process for ultrasensitive and recyclable detection of RhB. The uniform distribution of Cu<sub>2</sub>O shows two main roles in protecting AgNPs and providing CM effect. The Ag/Cu<sub>2</sub>O/ITO integrated sensitivity for SERS analysis (LOD of 1.0 pmol/L for RhB), long-term stability ( $\geq 58$  days), uniformity (RSD of 5.8% for 10 random points), and recyclability ( $\geq 10$  times), which exhibits great potentials in on-site monitoring of organic dyes. Das et al. [38] developed a large-scale paper-based membrane substrate for highly sensitive analysis R6G and RhB with LOD of 1.0 pmol/L and 1.0  $\mu\text{mol/L}$ , respectively. In addition, the as-fabricated membrane substrate shows satisfied reproducibility for SERS analysis of R6G and RhB in rain, pond, and tap water. A surface molecularly-imprinted magnetic solid substrate (Fe<sub>3</sub>O<sub>4</sub>@MIP) was constructed for trace analysis of MG in tap water and carp samples with low LOD of 1.50 and 1.62 pmol/L, respectively [126]. Combining magnetic core with molecularly imprinted layer endow effective and selective separation and enrichment of MG in complex samples. Considering the uniform distribution of magnetic solid substrate, the SERS signal of MG can be significantly enhanced after the transfer of Fe<sub>3</sub>O<sub>4</sub>@MIP on AgNPs deposited Si wafer.

Apart from organic dyes, there are several environmental pollutants have been detected successfully by solid substrate, such as PAHs [127], atmospheric aerosol [95,128], pesticide residues, drug residues [52,129,130], etc. The structure of solid SERS substrate can be designed and fabricated to meet requirement of SERS detection of environmental pollutants with high analytical performance. However, there are few environmental pollutants categories have been reported for SERS analysis based on solid substrate. Thus, the practical analysis of environmental pollutants based on solid SERS substrate still exhibits great development space, which need further exploring in the future.

#### 4.4. Other Analysis

The solid SERS substrates also have been applied to medicine and public safety analysis due to their portability, rapidity, sensitivity, and stability. White's [131] group developed a AgNPs printed paper membrane substrate for monitoring of therapeutic drug (flucytosine) with LOD of 10.0  $\mu\text{g/mL}$ . The developed membrane substrate combined with vertical-flow method can meet the requirement of rapid, on-site, and sensitive detection of flucytosine. Gupta et al. [132] fabricated a transparent and elastomeric film based on patched Au nanorods (AuNRs) modified PDMS for vapor-phase detection of explosives of trinitrotoluene (TNT). The as-fabricated film can realize the formation of dense hot spot by TNT capture process, indicating the large SERS enhancement. A solid substrate of AgNPs immobilized polyurethane sponge (PU@PDA@Ag) was constructed for trace SERS analysis of inorganic explosives including ClO<sup>4-</sup>, ClO<sup>3-</sup>, and NO<sup>3-</sup> [133]. The swabbing extraction

process significantly improve the collection efficiency and SERS performance. The LODs for  $\text{ClO}_4^-$ ,  $\text{ClO}_3^-$ , and  $\text{NO}_3^-$  were 0.012, 0.025 and 0.025  $\mu\text{mol/L}$  with high reproducible, stable and uniform SERS signals. The solid SERS substrate will play an important role in on-site, rapid and sensitive monitoring the illegal addition of drugs and illegal abuse of explosives.

## 5. Challenges and Perspectives

During past few years, it witnessed the flourishing development of solid SERS substrate in fabricating advanced substrate and broadening the scope of applications. Solid SERS substrates exhibit superiority in improvement of SERS analytical performance by dense hot spot, high stability, controllable morphology, and convenient portability. Furthermore, solid SERS substrate still shows great potentials in mass production and commercialization. However, despite above proposed advantages and superiorities, the solid SERS substrate also meets some challenges, mainly are improving the SERS analytical performance and enhancing the mass manufacture level.

The SERS analytical performance is the key parameters for analytical applications, which is mainly dependent on design and fabrication of solid SERS substrate. The analytical performance solid SERS substrate still need improved in four main aspects. First, how to precise control nanogap of plasmonic nanomaterials within few nanometers on the whole plane under the guidance of target size, which is the key to produce sensitive and uniform enhanced signals with high selectivity. Second, many reported solid SERS substrate meet limitations in terms of anti-interference ability for real samples, especially for pure plasmon based solid substrates. Third, the storage time of some solid SERS substrates still needs to be improved for SERS analysis, such as the paper-based membrane substrate, chip-based substrate, and magnetic solid substrate. Fourth, the scope of applications of solid SERS substrates is mainly in bio-analysis and food safety analysis, which should be expanded to more fields. In addition, the single molecule detection technology in nanocavities based on solid SERS substrates has drawn great attention due to its ultrahigh sensitivity, especially for nucleic acid detection [134–138]. However, the single molecule detection for other analytical fields remains in the initial stage, showing great prospects for development. Finally, choosing proper solid substrates for analytical applications (bio-analysis, food safety analysis and environment analysis) still meets limitations in diversification, demanding improvements to identify the best solid substrate for analytical applications. For example, the biocompatibility of solid SERS substrates for bio-analysis is still necessary.

At present, the fabrication of solid SERS substrates remains at the laboratory level, which limits their development in commercial applications. Thus, how to achieve the integration of batch production, long storage time, and commercialization all-in-one is significantly important for realizing practical applications. Hence, designing and fabricating a solid SERS substrate with excellent analytical performance combined with batch potential should be further investigated.

An ideal solid SERS substrate shows unique features in terms of promising enhancement effect, uniform and stable SERS signals, long storage time, and simple preparation process compared to common liquid SERS substrates. Converting from the traditional liquid SERS substrate to a novel solid SERS substrate provides a great opportunity to improve SERS performance and develop an effective commercialization platform. The solid SERS substrate will be a powerful tool for SERS analysis after addressing the challenges mentioned above.

**Author Contributions:** Conceptualization, K.G. and Y.H.; methodology, K.G., Y.H. and G.L.; formal analysis, K.G.; investigation, K.G.; resources, Y.H. and G.L.; data curation, K.G., Y.H. and G.L.; writing—original draft preparation, K.G.; writing—review and editing, K.G. and Y.H.; visualization, K.G.; supervision, Y.H.; project administration, Y.H. and G.L.; funding acquisition, Y.H. and G.L. All authors have read and agreed to the published version of the manuscript.

**Funding:** This research was funded by the National Natural Science Foundation of China (Nos.22074162), the Guangdong Provincial Natural Science Foundation of China (No.2022A1515011171), the National Key Research and Development Program of China (Nos.2018YFC1603201 and 2019YFC1606101), and the State Key Program of National Natural Science of China (No.22134007), respectively.

**Institutional Review Board Statement:** Not applicable.

**Informed Consent Statement:** Not applicable.

**Data Availability Statement:** The data presented in this study are available on request from the corresponding author.

**Conflicts of Interest:** The authors declare no conflict of interest.

## References

1. Cai, L.; Dong, J.; Wang, Y.; Chen, X. A review of developments and applications of thin-film microextraction coupled to surface-enhanced Raman scattering. *Electrophoresis* **2019**, *40*, 2041–2049. [[CrossRef](#)]
2. Zhang, D.; Liang, P.; Yu, Z.; Xia, J.; Ni, D.; Wang, D.; Zhou, Y.; Cao, Y.; Chen, J.; Chen, J.; et al. Self-assembled “bridge” substance for organochlorine pesticides detection in solution based on surface enhanced raman scattering. *J. Hazard. Mater.* **2020**, *382*, 121023. [[CrossRef](#)] [[PubMed](#)]
3. Deng, Z.; Chen, X.; Wang, Y.; Fang, E.; Zhang, Z.; Chen, X. Headspace thin-film microextraction coupled with surface-enhanced Raman scattering as a facile method for reproducible and specific detection of sulfur dioxide in wine. *Anal. Chem.* **2015**, *87*, 633–640. [[CrossRef](#)] [[PubMed](#)]
4. Zhang, C.Y.; Zhao, B.C.; Hao, R.; Wang, Z.; Hao, Y.W.; Zhao, B.; Liu, Y.Q. Graphene oxide-highly anisotropic noble metal hybrid systems for intensified surface enhanced Raman scattering and direct capture and sensitive discrimination in PCBs monitoring. *J. Hazard. Mater.* **2020**, *385*, 121510. [[CrossRef](#)] [[PubMed](#)]
5. Zhang, Z.; Wang, J.; Shanmugasundaram, K.B.; Yeo, B.; Moller, A.; Wuethrich, A.; Lin, L.L.; Trau, M. Tracking drug-induced epithelial-mesenchymal transition in breast cancer by a microfluidic surface-enhanced raman spectroscopy immunoassay. *Small* **2020**, *16*, e1905614. [[CrossRef](#)] [[PubMed](#)]
6. Lee, H.K.; Lee, Y.H.; Koh, C.S.L.; Phan-Quang, G.C.; Han, X.; Lay, C.L.; Sim, H.Y.F.; Kao, Y.C.; An, Q.; Ling, X.Y. Designing surface-enhanced Raman scattering (SERS) platforms beyond hotspot engineering: Emerging opportunities in analyte manipulations and hybrid materials. *Chem. Soc. Rev.* **2019**, *48*, 731–756. [[CrossRef](#)] [[PubMed](#)]
7. Zhan, C.; Chen, X.J.; Huang, Y.F.; Wu, D.Y.; Tian, Z.Q. Plasmon-mediated chemical reactions on nanostructures unveiled by surface-enhanced raman spectroscopy. *Acc. Chem. Res.* **2019**, *52*, 2784–2792. [[CrossRef](#)]
8. Karthick Kannan, P.; Shankar, P.; Blackman, C.; Chung, C.H. Recent advances in 2D inorganic nanomaterials for SERS sensing. *Adv. Mater.* **2019**, *31*, e1803432. [[CrossRef](#)]
9. Zhang, H.; Duan, S.; Radjenovic, P.M.; Tian, Z.Q.; Li, J.F. Core-shell nanostructure-enhanced raman spectroscopy for surface catalysis. *Acc. Chem. Res.* **2020**, *53*, 729–739. [[CrossRef](#)]
10. Hu, Y.; Liao, J.; Wang, D.; Li, G. Fabrication of gold nanoparticle-embedded metal-organic framework for highly sensitive surface-enhanced Raman scattering detection. *Anal. Chem.* **2014**, *86*, 955–963. [[CrossRef](#)]
11. Li, J.F.; Tian, X.D.; Li, S.B.; Anema, J.R.; Yang, Z.L.; Ding, Y.; Wu, Y.F.; Zeng, Y.M.; Chen, Q.Z.; Ren, B.; et al. Surface analysis using shell-isolated nanoparticle-enhanced Raman spectroscopy. *Nat. Protoc.* **2013**, *8*, 52–65. [[CrossRef](#)] [[PubMed](#)]
12. Renard, D.; Tian, S.; Ahmadiwand, A.; DeSantis, C.J.; Clark, B.D.; Nordlander, P.; Halas, N.J. Polydopamine-Stabilized Aluminum Nanocrystals: Aqueous Stability and Benzo[a]pyrene Detection. *ACS Nano* **2019**, *13*, 3117–3124. [[CrossRef](#)] [[PubMed](#)]
13. Phan-Quang, G.C.; Yang, N.; Lee, H.K.; Sim, H.Y.F.; Koh, C.S.L.; Kao, Y.C.; Wong, Z.C.; Tan, E.K.M.; Miao, Y.E.; Fan, W.; et al. Tracking airborne molecules from afar: Three-dimensional metal-organic framework-surface-enhanced Raman scattering platform for stand-off and real-time atmospheric monitoring. *ACS Nano* **2019**, *13*, 12090–12099. [[CrossRef](#)] [[PubMed](#)]
14. Carrillo-Carrion, C.; Martinez, R.; Navarro Poupard, M.F.; Pelaz, B.; Polo, E.; Arenas-Vivo, A.; Olgiati, A.; Taboada, P.; Soliman, M.G.; Catalan, U.; et al. Aqueous stable gold nanostar/ZIF-8 nanocomposites for light-triggered release of active cargo inside living cells. *Angew. Chem. Int. Ed.* **2019**, *58*, 7078–7082. [[CrossRef](#)] [[PubMed](#)]
15. Liu, J.; Zheng, T.; Tian, Y. Functionalized h-BN nanosheets as a Theranostic platform for SERS real-time monitoring of MicroRNA and photodynamic therapy. *A Angew. Chem. Int. Ed.* **2019**, *58*, 7757–7761. [[CrossRef](#)]
16. Quan, J.; Zhang, J.; Li, J.; Zhang, X.; Wang, M.; Wang, N.; Zhu, Y. Three-dimensional AgNPs-graphene-AgNPs sandwiched hybrid nanostructures with sub-nanometer gaps for ultrasensitive surface-enhanced Raman spectroscopy. *Carbon* **2019**, *147*, 105–111. [[CrossRef](#)]
17. Chen, Y.; Zhang, Y.; Pan, F.; Liu, J.; Wang, K.; Zhang, C.; Cheng, S.; Lu, L.; Zhang, W.; Zhang, Z.; et al. Breath analysis based on surface-enhanced Raman scattering sensors distinguishes early and advanced gastric cancer patients from healthy persons. *ACS Nano* **2016**, *10*, 8169–8179. [[CrossRef](#)]
18. Tang, W.; An, Y.; Ho Row, K. Fabrication of Au nanoparticles embedded holey g-C<sub>3</sub>N<sub>4</sub> as SERS substrates for sensitive and reliable detection. *Chem. Eng. J.* **2020**, *402*, 126194. [[CrossRef](#)]

19. Martins, N.C.T.; Fateixa, S.; Fernandes, T.; Nogueira, H.I.S.; Trindade, T. Inkjet printing of Ag and polystyrene nanoparticle emulsions for the one-step fabrication of hydrophobic paper-based surface-enhanced Raman scattering substrates. *ACS Appl. Nano Mater.* **2021**, *4*, 4484–4495. [[CrossRef](#)]
20. Duan, J.; Qiu, Z.; Li, L.; Feng, L.; Huang, L.; Xiao, G. Inkjet printed silver nanoparticles on hydrophobic papers for efficient detection of thiram. *Spectrochim. Acta A* **2020**, *243*, 118811. [[CrossRef](#)]
21. Pan, X.; Li, L.; Lin, H.; Tan, J.; Wang, H.; Liao, M.; Chen, C.; Shan, B.; Chen, Y.; Li, M. A graphene oxide-gold nanostar hybrid based-paper biosensor for label-free SERS detection of serum bilirubin for diagnosis of jaundice. *Biosens. Bioelectron.* **2019**, *145*, 111713. [[CrossRef](#)] [[PubMed](#)]
22. Lei, H.; Hu, Y.; Li, G. A dual-functional membrane for bisphenol A enrichment and resonance amplification by surface-enhanced Raman scattering. *Chin. Chem. Lett.* **2018**, *29*, 509–512. [[CrossRef](#)]
23. Li, J.; Yi, W.; Li, Y.; Liu, W.; Bai, H.; Jiao, Z.; Zhang, Y.; Wang, X.; Zou, M.; Xi, G. Nitrogen-doped titanium monoxide flexible membrane for a low-cost, biocompatible, and durable Raman scattering substrate. *Anal. Chem.* **2021**, *93*, 12776–12785. [[CrossRef](#)]
24. Cao, Z.; He, P.; Huang, T.; Yang, S.; Han, S.; Wang, X.; Ding, G. Plasmonic coupling of AgNPs near graphene edges: A cross-section strategy for high-performance SERS sensing. *Chem. Mater.* **2020**, *32*, 3813–3822. [[CrossRef](#)]
25. Lim, S.H.; Lee, M.J.; Kang, S.H.; Dey, J.; Umar, A.; Lee, S.J.; Choi, S.M. Individually silica-embedded gold nanorod superlattice for high thermal and solvent stability and recyclable SERS application. *Adv. Mater. Interfaces* **2019**, *6*, 1900986. [[CrossRef](#)]
26. Xing, C.; Liu, D.; Chen, J.; Fan, Y.; Zhou, F.; Kaur, K.; Cai, W.; Li, Y. Convective self-assembly of 2D nonclose-packed binary au nanoparticle arrays with tunable optical properties. *Chem. Mater.* **2020**, *33*, 310–319. [[CrossRef](#)]
27. Wang, K.; Sun, D.W.; Pu, H.; Wei, Q. Two-dimensional Au@Ag nanodot array for sensing dual-fungicides in fruit juices with surface-enhanced Raman spectroscopy technique. *Food Chem.* **2020**, *310*, 125923. [[CrossRef](#)]
28. Kim, S.; Kim, T.G.; Lee, S.H.; Kim, W.; Bang, A.; Moon, S.W.; Song, J.; Shin, J.H.; Yu, J.S.; Choi, S. Label-free surface-enhanced raman spectroscopy biosensor for on-site breast cancer detection using human tears. *ACS Appl. Mater. Interfaces* **2020**, *12*, 7897–7904. [[CrossRef](#)]
29. Zhu, A.; Zhao, X.; Cheng, M.; Chen, L.; Wang, Y.; Zhang, X.; Zhang, Y.; Zhang, X. Nanohoneycomb surface-enhanced raman spectroscopy-active chip for the determination of biomarkers of hepatocellular carcinoma. *ACS Appl. Mater. Interfaces* **2019**, *11*, 44617–44623. [[CrossRef](#)]
30. Huang, J.; He, Z.; Liu, Y.; Liu, L.; He, X.; Wang, T.; Yi, Y.; Xie, C.; Du, K. Large surface-enhanced Raman scattering from nanoporous gold film over nanosphere. *Appl. Surf. Sci.* **2019**, *478*, 793–801. [[CrossRef](#)]
31. Castro-Grijalba, A.; Montes-Garcia, V.; Cordero-Ferradas, M.J.; Coronado, E.; Perez-Juste, J.; Pastoriza-Santos, I. SERS-based molecularly imprinted plasmonic sensor for highly sensitive PAH detection. *ACS Sens.* **2020**, *5*, 693–702. [[CrossRef](#)] [[PubMed](#)]
32. Zhao, B.; Hao, R.; Wang, Z.; Zhang, H.; Hao, Y.; Zhang, C.; Liu, Y. Green synthesis of multi-dimensional plasmonic coupling structures: Graphene oxide gapped gold nanostars for highly intensified surface enhanced Raman scattering. *Chem. Eng. J.* **2018**, *349*, 581–587. [[CrossRef](#)]
33. Li, J.; Yan, H.; Tan, X.; Lu, Z.; Han, H. Cauliflower-inspired 3D SERS substrate for multiple mycotoxins detection. *Anal. Chem.* **2019**, *91*, 3885–3892. [[CrossRef](#)] [[PubMed](#)]
34. Shi, G.; Wang, M.; Zhu, Y.; Wang, Y.; Xu, H. A novel natural SERS system for crystal violet detection based on graphene oxide wrapped Ag micro-islands substrate fabricated from Lotus leaf as a template. *Appl. Surf. Sci.* **2018**, *459*, 802–811. [[CrossRef](#)]
35. Cai, Z.; Hu, Y.; Sun, Y.; Gu, Q.; Wu, P.; Cai, C.; Yan, Z. Plasmonic SERS Biosensor Based on Multibranching Gold Nanoparticles Embedded in Polydimethylsiloxane for Quantification of Hematin in Human Erythrocytes. *Anal. Chem.* **2021**, *93*, 1025–1032. [[CrossRef](#)] [[PubMed](#)]
36. Panikar, S.S.; Ramirez-Garcia, G.; Sidhik, S.; Lopez-Luke, T.; Rodriguez-Gonzalez, C.; Ciapara, I.H.; Castillo, P.S.; Camacho-Villegas, T.; De la Rosa, E. Ultrasensitive SERS substrate for label-free therapeutic-drug monitoring of paclitaxel and cyclophosphamide in blood serum. *Anal. Chem.* **2019**, *91*, 2100–2111. [[CrossRef](#)]
37. Ge, K.; Hu, Y.; Zheng, Y.; Jiang, P.; Li, G. Aptamer/derivatization-based surface-enhanced Raman scattering membrane assembly for selective analysis of melamine and formaldehyde in migration of melamine kitchenware. *Talanta* **2021**, *235*, 122743. [[CrossRef](#)]
38. Das, D.; Senapati, S.; Nanda, K.K. “Rinse, repeat”: An efficient and reusable SERS and catalytic platform fabricated by controlled deposition of silver nanoparticles on cellulose paper. *Sustain. Chem. Eng.* **2019**, *7*, 14089–14101. [[CrossRef](#)]
39. Yilmaz, H.; Bae, S.H.; Cao, S.; Wang, Z.; Raman, B.; Singamaneni, S. Gold-nanorod-based plasmonic nose for analysis of chemical mixtures. *ACS Appl. Nano Mater.* **2019**, *2*, 3897–3905. [[CrossRef](#)]
40. Kumar, A.; Santhanam, V. Paper swab based SERS detection of non-permitted colourants from dals and vegetables using a portable spectrometer. *Anal. Chim. Acta* **2019**, *1090*, 106–113. [[CrossRef](#)]
41. Zhang, C.; You, T.; Yang, N.; Gao, Y.; Jiang, L.; Yin, P. Hydrophobic paper-based SERS platform for direct-droplet quantitative determination of melamine. *Food Chem.* **2019**, *287*, 363–368. [[CrossRef](#)] [[PubMed](#)]
42. Kim, D.; Ko, Y.; Kwon, G.; Choo, Y.-M.; You, J. Low-cost, high-performance plasmonic nanocomposites for hazardous chemical detection using surface enhanced Raman scattering. *Sens. Actuat. B Chem.* **2018**, *274*, 30–36. [[CrossRef](#)]
43. Huang, D.; Zhuang, Z.; Wang, Z.; Li, S.; Zhong, H.; Liu, Z.; Guo, Z.; Zhang, W. Black phosphorus-Au filter paper-based three-dimensional SERS substrate for rapid detection of foodborne bacteria. *Appl. Surf. Sci.* **2019**, *497*, 143825. [[CrossRef](#)]
44. Fu, J.; Lai, H.; Zhang, Z.; Li, G. UiO-66 metal-organic frameworks/gold nanoparticles based substrates for SERS analysis of food samples. *Anal. Chim. Acta* **2021**, *1161*, 338464. [[CrossRef](#)]

45. Ge, K.; Hu, Y.; Li, G. Fabrication of branched gold copper nanoalloy doped mesoporous graphitic carbon nitride hybrid membrane for surface-enhanced Raman spectroscopy analysis of carcinogens. *J. Hazard. Mater.* **2022**, *432*, 128742. [[CrossRef](#)]
46. Kim, H.; Trinh, B.T.; Kim, K.H.; Moon, J.; Kang, H.; Jo, K.; Akter, R.; Jeong, J.; Lim, E.K.; Jung, J.; et al. Au@ZIF-8 SERS paper for food spoilage detection. *Biosens. Bioelectron.* **2021**, *179*, 113063. [[CrossRef](#)]
47. Yang, Z.; Liu, H.; Tian, Y.; Chen, Y.; Niu, Z.; Zhou, C.; Wang, F.; Gu, C.; Tang, S.; Jiang, T.; et al. Synergistic effect of a “stellate” mesoporous SiO<sub>2</sub>@Au nanoprobe and coffee-ring-free hydrophilic–hydrophobic substrate assembly in an ultrasensitive SERS-based immunoassay for a tumor marker. *J. Mater. Chem. C* **2020**, *8*, 2142–2154. [[CrossRef](#)]
48. Zou, Y.; Zhang, Y.; Xu, Y.; Chen, Y.; Huang, S.; Lyu, Y.; Duan, H.; Chen, Z.; Tan, W. Portable and label-free detection of blood bilirubin with graphene-isolated-au-nanocrystals paper strip. *Anal. Chem.* **2018**, *90*, 13687–13694. [[CrossRef](#)]
49. Yu, Z.; Huang, L.; Zhang, Z.; Li, G. Simultaneous and accurate quantification of multiple antibiotics in aquatic samples by surface-enhanced raman scattering using a Ti<sub>3</sub>C<sub>2</sub>T<sub>x</sub>/DNA/Ag membrane substrate. *Anal. Chem.* **2021**, *93*, 13072–13079. [[CrossRef](#)]
50. Wu, S.; Duan, N.; Shen, M.; Wang, J.; Wang, Z. Surface-enhanced Raman spectroscopic single step detection of *Vibrio parahaemolyticus* using gold coated polydimethylsiloxane as the active substrate and aptamer modified gold nanoparticles. *Microchim. Acta* **2019**, *186*, 401. [[CrossRef](#)]
51. Ma, Y.; Liu, H.; Chen, Y.; Du, Y.; Gu, C.; Zhao, Z.; Si, H.; Wei, G.; Jiang, T.; Zhou, J. Quantitative and recyclable surface-enhanced raman spectroscopy immunoassay based on Fe<sub>3</sub>O<sub>4</sub>@TiO<sub>2</sub>@Ag core–shell nanoparticles and au nanowire/polydimethylsiloxane substrates. *ACS Appl. Nano Mater.* **2020**, *3*, 4610–4622. [[CrossRef](#)]
52. Wang, M.; Wang, Y.; Qiao, Y.; Wei, M.; Gao, L.; Wang, L.; Yan, Y.; Li, H. High-sensitive imprinted membranes based on surface-enhanced Raman scattering for selective detection of antibiotics in water. *Spectrochim. Acta A* **2019**, *222*, 117116. [[CrossRef](#)] [[PubMed](#)]
53. Guo, J.; Zhong, Z.; Li, Y.; Liu, Y.; Wang, R.; Ju, H. “Three-in-one” SERS adhesive tape for rapid sampling, release, and detection of wound infectious pathogens. *ACS Appl. Mater. Interfaces* **2019**, *11*, 36399–36408. [[CrossRef](#)] [[PubMed](#)]
54. Yao, Y.; Ji, J.; Zhang, H.; Zhang, K.; Liu, B.; Yang, P. Three-Dimensional plasmonic trap array for ultrasensitive surface-enhanced Raman scattering analysis of single cells. *Anal. Chem.* **2018**, *90*, 10394–10399. [[CrossRef](#)] [[PubMed](#)]
55. Qu, L.; Wang, N.; Xu, H.; Wang, W.; Liu, Y.; Kuo, L.; Yadav, T.P.; Wu, J.; Joyner, J.; Song, Y.; et al. Gold nanoparticles and g-C<sub>3</sub>N<sub>4</sub>-intercalated graphene oxide membrane for recyclable surface enhanced Raman scattering. *Adv. Funct. Mater.* **2017**, *27*, 1701714. [[CrossRef](#)]
56. Guan, H.; Yi, W.; Li, T.; Li, Y.; Li, J.; Bai, H.; Xi, G. Low temperature synthesis of plasmonic molybdenum nitride nanosheets for surface enhanced Raman scattering. *Nat. Commun.* **2020**, *11*, 3889. [[CrossRef](#)]
57. Hanske, C.; Hill, E.H.; Vila-Liarte, D.; Gonzalez-Rubio, G.; Matricardi, C.; Mihi, A.; Liz-Marzan, L.M. Solvent-assisted self-assembly of gold nanorods into hierarchically organized plasmonic mesostructures. *ACS Appl. Mater. Interfaces* **2019**, *11*, 11763–11771. [[CrossRef](#)]
58. Zhang, H.; Wang, R.; Sikdar, D.; Wu, L.; Sun, J.; Gu, N.; Chen, Y. Plasmonic superlattice membranes based on bimetallic nano-sea urchins as high-performance label-free surface-enhanced Raman spectroscopy platforms. *ACS Sens.* **2022**, *7*, 622–631. [[CrossRef](#)]
59. Tian, T.; Yi, J.; Liu, Y.; Li, B.; Liu, Y.; Qiao, L.; Zhang, K.; Liu, B. Self-assembled plasmonic nanoarrays for enhanced bacterial identification and discrimination. *Biosens. Bioelectron.* **2022**, *197*, 113778. [[CrossRef](#)]
60. Deng, Z.; Wen, P.; Wang, N.; Peng, B. Preparation of hierarchical superhydrophobic melamine-formaldehyde/Ag nanocomposite arrays as surface-enhanced Raman scattering substrates for ultrasensitive and reproducible detection of biomolecules. *Sens. Actuat. B Chem.* **2019**, *288*, 20–26. [[CrossRef](#)]
61. Mao, P.; Liu, C.; Favraud, G.; Chen, Q.; Han, M.; Fratolocchi, A.; Zhang, S. Broadband single molecule SERS detection designed by warped optical spaces. *Nat. Commun.* **2018**, *9*, 5428. [[CrossRef](#)]
62. Dong, S.; Wang, Y.; Liu, Z.; Zhang, W.; Yi, K.; Zhang, X.; Zhang, X.; Jiang, C.; Yang, S.; Wang, F.; et al. Beehive-inspired macroporous SERS probe for cancer detection through capturing and analyzing exosomes in plasma. *ACS Appl. Mater. Interfaces* **2020**, *12*, 5136–5146. [[CrossRef](#)]
63. Zukovskaja, O.; Agafilushkina, S.; Sivakov, V.; Weber, K.; Cialla-May, D.; Osminkina, L.; Popp, J. Rapid detection of the bacterial biomarker pyocyanin in artificial sputum using a SERS-active silicon nanowire matrix covered by bimetallic noble metal nanoparticles. *Talanta* **2019**, *202*, 171–177. [[CrossRef](#)] [[PubMed](#)]
64. Feng, L.; Wang, W.; Li, X.; Chen, T. Spontaneous growth of 3D silver mesoflowers on poly(4-vinylpyridine) brushes-grafted-graphene oxide films and facile creation of nanoporosities over their surface. *Chemistry* **2019**, *25*, 16377–16381. [[CrossRef](#)] [[PubMed](#)]
65. Li, C.; Liu, Y.; Zhou, X.; Wang, Y. A paper-based SERS assay for sensitive duplex cytokine detection towards the atherosclerosis-associated disease diagnosis. *J. Mater. Chem. B* **2019**, *8*, 582–589. [[CrossRef](#)] [[PubMed](#)]
66. Lin, B.; Chen, J.; Kannan, P.; Zeng, Y.; Qiu, B.; Guo, L.; Lin, Z. Rapid synthesis of a highly active and uniform 3-dimensional SERS substrate for on-spot sensing of dopamine. *Microchim. Acta* **2019**, *186*, 60. [[CrossRef](#)]
67. Liu, Y.; Liu, Y.; Xing, Y.; Guo, X.; Ying, Y.; Wu, Y.; Wen, Y.; Yang, H. Magnetically three-dimensional Au nanoparticles/reduced graphene/ nickel foams for Raman trace detection. *Sens. Actuat. B Chem.* **2018**, *273*, 884–890. [[CrossRef](#)]
68. Zhou, Y.; Li, J.; Zhang, L.; Ge, Z.; Wang, X.; Hu, X.; Xu, T.; Li, P.; Xu, W. HS-beta-cyclodextrin-functionalized Ag@Fe<sub>3</sub>O<sub>4</sub>@Ag nanoparticles as a surface-enhanced Raman spectroscopy substrate for the sensitive detection of butyl benzyl phthalate. *Anal. Bioanal. Chem.* **2019**, *411*, 5691–5701. [[CrossRef](#)]

69. Zhang, H.; Lai, H.; Wu, X.; Li, G.; Hu, Y. CoFe<sub>2</sub>O<sub>4</sub>@HNTs/AuNPs Substrate for rapid magnetic solid-phase extraction and efficient SERS detection of complex samples all-in-one. *Anal. Chem.* **2020**, *92*, 4607–4613. [[CrossRef](#)]
70. Witkowska, E.; Lasica, A.M.; Nicinski, K.; Potempa, J.; Kaminska, A. In search of spectroscopic signatures of Periodontitis: A SERS-based magnetofluidic sensor for detection of *Porphyromonas gingivalis* and *Aggregatibacter actinomycetemcomitans*. *ACS Sens.* **2021**, *6*, 1621–1635. [[CrossRef](#)]
71. Kim, H.; Lee, S.; Seo, H.W.; Kang, B.; Moon, J.; Lee, K.G.; Yong, D.; Kang, H.; Jung, J.; Lim, E.K.; et al. Clustered regularly interspaced short palindromic repeats-mediated surface-enhanced Raman scattering assay for multidrug-resistant bacteria. *ACS Nano* **2020**, *14*, 17241–17253. [[CrossRef](#)] [[PubMed](#)]
72. Wu, J.; Zhou, X.; Li, P.; Lin, X.; Wang, J.; Hu, Z.; Zhang, P.; Chen, D.; Cai, H.; Niessner, R.; et al. Ultrasensitive and simultaneous SERS Detection of multiplex MicroRNA using fractal gold nanotags for early diagnosis and prognosis of Hepatocellular Carcinoma. *Anal. Chem.* **2021**, *93*, 8799–8809. [[CrossRef](#)] [[PubMed](#)]
73. Jung, H.S.; Koh, E.H.; Mun, C.; Min, J.; Sohng, W.; Chung, H.; Yang, J.-Y.; Lee, S.; Kim, H.J.; Park, S.-G.; et al. Hydrophobic hBN-coated surface-enhanced Raman scattering sponge sensor for simultaneous separation and detection of organic pollutants. *J. Mater. Chem. C* **2019**, *7*, 13059–13069. [[CrossRef](#)]
74. Zhou, B.; Shen, J.; Li, P.; Ge, M.; Lin, D.; Li, Y.Y.; Lu, J.; Yang, L. Gold nanoparticle-decorated silver needle for surface-enhanced Raman spectroscopy screening of residual malachite green in aquaculture products. *ACS Appl. Nano Mater.* **2019**, *2*, 2752–2757. [[CrossRef](#)]
75. Ankudze, B.; Asare, B.; Goffart, S.; Koistinen, A.; Nuutinen, T.; Matikainen, A.; Andoh, S.S.; Roussey, M.; Pakkanen, T.T. Hydraulically pressed silver nanowire-cotton fibers as an active platform for filtering and surface-enhanced Raman scattering detection of bacteria from fluid. *Appl. Surf. Sci.* **2019**, *479*, 663–668. [[CrossRef](#)]
76. Park, S.; Lee, J.; Ko, H. Transparent and Flexible Surface-Enhanced Raman Scattering (SERS) sensors based on gold nanostar arrays embedded in silicon rubber film. *ACS Appl. Mater. Interfaces* **2017**, *9*, 44088–44095. [[CrossRef](#)]
77. Ma, Y.; Chen, Y.; Tian, Y.; Gu, C.; Jiang, T. Contrastive Study of in situ sensing and swabbing detection based on SERS-active gold nanobush-PDMS hybrid film. *J. Agric. Food Chem.* **2021**, *69*, 1975–1983. [[CrossRef](#)]
78. Zhang, L.; Li, X.; Liu, W.; Hao, R.; Jia, H.; Dai, Y.; Usman Amin, M.; You, H.; Li, T.; Fang, J. Highly active Au NP microarray films for direct SERS detection. *J. Mater. Chem. C* **2019**, *7*, 15259–15268. [[CrossRef](#)]
79. Li, L.; Chin, W.S. Rapid fabrication of a flexible and transparent Ag nanocubes@PDMS film as a SERS substrate with high performance. *ACS Appl. Mater. Interfaces* **2020**, *12*, 37538–37548. [[CrossRef](#)]
80. Ma, Y.; Du, Y.; Chen, Y.; Gu, C.; Jiang, T.; Wei, G.; Zhou, J. Intrinsic Raman signal of polymer matrix induced quantitative multiphase SERS analysis based on stretched PDMS film with anchored Ag nanoparticles/Au nanowires. *Chem. Eng. J.* **2020**, *381*, 122710. [[CrossRef](#)]
81. Li, X.; Liu, H.; Gu, C.; Zhang, J.; Jiang, T. PDMS/TiO<sub>2</sub>/Ag hybrid substrate with intrinsic signal and clean surface for recyclable and quantitative SERS sensing. *Sens. Actuat. B Chem.* **2022**, *351*, 130886. [[CrossRef](#)]
82. Li, H.; Dai, H.; Zhang, Y.; Lee, Y.H.; Koh, C.S.L.; Phan-Quang, G.C.; Tong, W.; Zhang, Y.; Gao, H.; Ling, X.Y.; et al. Triboelectrically boosted SERS on sea-urchin-like gold clusters facilitated by a high dielectric substrate. *Nano Energy* **2019**, *64*, 130959. [[CrossRef](#)]
83. Li, H.; Dai, H.; Zhang, Y.; Tong, W.; Gao, H.; An, Q. Surface-enhanced Raman spectra promoted by a finger press in an all-solid-state flexible energy conversion and storage film. *Angew. Chem. Int. Ed.* **2017**, *56*, 2649–2654. [[CrossRef](#)] [[PubMed](#)]
84. Qiu, H.; Guo, J.; Wang, M.; Ji, S.; Cao, M.; Padhiar, M.A.; Bhatti, A.S. Reduced graphene oxide supporting Ag meso-flowers and phenyl-modified graphitic carbon nitride as self-cleaning flexible SERS membrane for molecular trace-detection. *Colloid. Surface. A* **2019**, *560*, 9–19. [[CrossRef](#)]
85. Song, X.; Yi, W.; Li, J.; Kong, Q.; Bai, H.; Xi, G. Selective Preparation of Mo<sub>2</sub>N and MoN with High Surface Area for Flexible SERS Sensing. *Nano Lett.* **2021**, *21*, 4410–4414. [[CrossRef](#)] [[PubMed](#)]
86. Wang, H.; Yao, L.; Mao, X.; Wang, K.; Zhu, L.; Zhu, J. Gold nanoparticle superlattice monolayer with tunable interparticle gap for surface-enhanced Raman spectroscopy. *Nanoscale* **2019**, *11*, 13917–13923. [[CrossRef](#)] [[PubMed](#)]
87. Hu, B.; Sun, D.W.; Pu, H.; Wei, Q. Rapid nondestructive detection of mixed pesticides residues on fruit surface using SERS combined with self-modeling mixture analysis method. *Talanta* **2020**, *217*, 120998. [[CrossRef](#)]
88. Kim, J.; Song, X.; Ji, F.; Luo, B.; Ice, N.F.; Liu, Q.; Zhang, Q.; Chen, Q. Polymorphic assembly from beveled gold triangular nanoprisms. *Nano Lett.* **2017**, *17*, 3270–3275. [[CrossRef](#)]
89. Karabel Ocal, S.; Patarroyo, J.; Kiremitler, N.B.; Pekdemir, S.; Puentes, V.F.; Onses, M.S. Plasmonic assemblies of gold nanorods on nanoscale patterns of poly(ethylene glycol): Application in surface-enhanced Raman spectroscopy. *J. Colloid. Interface Sci.* **2018**, *532*, 449–455. [[CrossRef](#)]
90. Velazquez-Salazar, J.J.; Bazan-Diaz, L.; Zhang, Q.; Mendoza-Cruz, R.; Montano-Priede, L.; Guisbiers, G.; Large, N.; Link, S.; Jose-Yacaman, M. Controlled overgrowth of five-fold concave nanoparticles into plasmonic nanostars and their single-particle scattering properties. *ACS Nano* **2019**, *13*, 10113–10128. [[CrossRef](#)]
91. Zhang, Z.; Bando, K.; Mochizuki, K.; Taguchi, A.; Fujita, K.; Kawata, S. Quantitative evaluation of surface-enhanced Raman scattering nanoparticles for intracellular pH sensing at a single particle level. *Anal. Chem.* **2019**, *91*, 53254–53262. [[CrossRef](#)] [[PubMed](#)]
92. Fang, X.; Zheng, C.; Yin, Z.; Wang, Z.; Wang, J.; Liu, J.; Luo, D.; Liu, Y.J. Hierarchically ordered silicon metastructures from improved self-assembly-based nanosphere lithography. *ACS Appl. Mater. Interfaces* **2020**, *12*, 12345–12352. [[CrossRef](#)] [[PubMed](#)]

93. Yang, H.; Li, B.Q.; Jiang, X.; Shao, J. Hybrid nanostructure of SiO<sub>2</sub>@Si with Au-nanoparticles for surface enhanced Raman spectroscopy. *Nanoscale* **2019**, *11*, 13484–13493. [[CrossRef](#)] [[PubMed](#)]
94. Guan, Y.; Wang, Z.; Gu, P.; Wang, Y.; Zhang, W.; Zhang, G. An in situ SERS study of plasmonic nanochemistry based on bifunctional “hedgehog-like” arrays. *Nanoscale* **2019**, *11*, 9422–9428. [[CrossRef](#)]
95. Dong, X.; Ohnoutek, L.; Yang, Y.; Feng, Y.; Wang, T.; Tahir, M.A.; Valev, V.K.; Zhang, L. Cu/Ag sphere segment void array as efficient surface enhanced Raman spectroscopy substrate for detecting individual atmospheric aerosol. *Anal. Chem.* **2019**, *91*, 13647–13657. [[CrossRef](#)]
96. Zhu, A.; Zhang, F.; Gao, R.; Zhao, X.; Chen, L.; Zhang, Y.; Zhang, X.; Wang, Y. Increasing polarization-dependent SERS effects by optimizing the axial symmetry of plasmonic nanostructures. *Appl. Surf. Sci.* **2019**, *494*, 87–93. [[CrossRef](#)]
97. Nie, B.; Luo, Y.; Shi, J.; Gao, L.; Duan, G. Bowl-like Pore array made of hollow Au/Ag alloy nanoparticles for SERS detection of melamine in solid milk powder. *Sens. Actuat. B Chem.* **2019**, *301*, 127087. [[CrossRef](#)]
98. Zhang, X.; Zhang, X.; Luo, C.; Liu, Z.; Chen, Y.; Dong, S.; Jiang, C.; Yang, S.; Wang, F.; Xiao, X. Volume-enhanced Raman scattering detection of viruses. *Small* **2019**, *15*, e1805516. [[CrossRef](#)]
99. Meng, T.; Shi, M.; Guo, Y.; Wang, H.; Fu, N.; Liu, Z.; Huang, B.; Lei, C.; Su, X.; Peng, B.; et al. Multifunctional Ag-coated CuO microbowl arrays for highly efficient, ultrasensitive, and recyclable surface-enhanced Raman scattering. *Sens. Actuat. B Chem.* **2022**, *354*, 131097. [[CrossRef](#)]
100. Liu, Y.; Luo, F. Large-scale highly ordered periodic Au nano-discs/graphene and graphene/Au nanoholes plasmonic substrates for surface-enhanced Raman scattering. *Nano Res.* **2019**, *12*, 2788–2795. [[CrossRef](#)]
101. Kim, N.; Thomas, M.R.; Bergholt, M.S.; Pence, I.J.; Seong, H.; Charchar, P.; Todorova, N.; Nagelkerke, A.; Belessiotis-Richards, A.; Payne, D.J.; et al. Surface enhanced Raman scattering artificial nose for high dimensionality fingerprinting. *Nat. Commun.* **2020**, *11*, 207. [[CrossRef](#)] [[PubMed](#)]
102. Zhang, M.; Sun, H.; Chen, X.; Yang, J.; Shi, L.; Chen, T.; Bao, Z.; Liu, J.; Wu, Y. Highly efficient Photoinduced Enhanced Raman Spectroscopy (PIERS) from plasmonic nanoparticles decorated 3D Semiconductor arrays for ultrasensitive, portable, and recyclable detection of organic pollutants. *ACS Sens.* **2019**, *4*, 1670–1681. [[CrossRef](#)] [[PubMed](#)]
103. Gao, Y.; You, T.; Yang, N.; Zhang, C.; Yin, P. Superhydrophobic 3D forest-like Ag microball/nanodendrite hierarchical structure as SERS sensor for rapid droplets detection. *Adv. Mater. Inter.* **2019**, *6*, 1801966. [[CrossRef](#)]
104. Mhlanga, N.; Domfe, T.; Skepu, A. Fabrication of surface enhanced Raman spectroscopy substrates on solid supports. *Appl. Surf. Sci.* **2019**, *476*, 1108–1117. [[CrossRef](#)]
105. Zhu, Y.; Wu, L.; Yan, H.; Lu, Z.; Yin, W.; Han, H. Enzyme induced molecularly imprinted polymer on SERS substrate for ultrasensitive detection of patulin. *Anal. Chim. Acta* **2020**, *1101*, 111–119. [[CrossRef](#)]
106. Kim, N.Y.; Leem, Y.C.; Hong, S.H.; Park, J.H.; Yim, S.Y. Ultrasensitive and stable plasmonic surface-enhanced Raman scattering substrates covered with atomically thin monolayers: Effect of the insulating property. *ACS Appl. Mater. Interfaces* **2019**, *11*, 6363–6373. [[CrossRef](#)]
107. Li, Y.; Duan, W.; Wei, J. CoFe<sub>2</sub>O<sub>4</sub>/Ag Nanostructures as highly sensitive surface-enhanced Raman scattering substrates. *ACS Appl. Nano Mater.* **2021**, *4*, 4181–4188. [[CrossRef](#)]
108. Ma, X.; Wen, S.; Xue, X.; Guo, Y.; Jin, J.; Song, W.; Zhao, B. Controllable synthesis of SERS-active magnetic metal-organic framework-based nanocatalysts and their application in photoinduced enhanced catalytic oxidation. *ACS Appl. Mater. Interfaces* **2018**, *10*, 25726–25736. [[CrossRef](#)]
109. Chattopadhyay, S.; Sabharwal, P.K.; Jain, S.; Kaur, A.; Singh, H. Functionalized polymeric magnetic nanoparticle assisted SERS immunosensor for the sensitive detection of *S. typhimurium*. *Anal. Chim. Acta* **2019**, *1067*, 98–106. [[CrossRef](#)]
110. Xu, Y.; Hassan, M.M.; Ali, S.; Li, H.; Chen, Q. SERS-based rapid detection of 2,4-dichlorophenoxyacetic acid in food matrices using molecularly imprinted magnetic polymers. *Microchim. Acta* **2020**, *187*, 454. [[CrossRef](#)]
111. Huang, W.-R.; Yu, C.-X.; Lu, Y.-R.; Muhammad, H.; Wang, J.-L.; Liu, J.-W.; Yu, S.-H. Mass-production of flexible and transparent Te-Au nylon SERS substrate with excellent mechanical stability. *Nano Res.* **2019**, *12*, 1483–1488. [[CrossRef](#)]
112. Ding, Q.; Kang, Z.; He, X.; Wang, M.; Lin, M.; Lin, H.; Yang, D.P. Eggshell membrane-templated gold nanoparticles as a flexible SERS substrate for detection of thiabendazole. *Mikrochim. Acta* **2019**, *186*, 453. [[CrossRef](#)] [[PubMed](#)]
113. Wang, Y.; Zhang, M.; Feng, L.; Dong, B.; Xu, T.; Li, D.; Jiang, L.; Chi, L. Tape-Imprinted Hierarchical Lotus Seedpod-Like Arrays for Extraordinary Surface-Enhanced Raman Spectroscopy. *Small* **2019**, *15*, e1804527. [[CrossRef](#)] [[PubMed](#)]
114. Lu, S.; Du, J.; Sun, Z.; Jing, C. Hairpin-structured magnetic SERS sensor for tetracycline resistance gene tetA detection. *Anal. Chem.* **2020**, *92*, 16229–16235. [[CrossRef](#)] [[PubMed](#)]
115. Zhao, W.; Zhang, D.; Zhou, T.; Huang, J.; Wang, Y.; Li, B.; Chen, L.; Yang, J.; Liu, Y. Aptamer-conjugated magnetic Fe<sub>3</sub>O<sub>4</sub>@Au core-shell multifunctional nanoprobe: A three-in-one aptasensor for selective capture, sensitive SERS detection and efficient near-infrared light triggered photothermal therapy of *Staphylococcus aureus*. *Sens. Actuat. B Chem.* **2022**, *350*, 130879. [[CrossRef](#)]
116. Jalalvand, A.R. Fabrication of a novel and high-performance amperometric sensor for highly sensitive determination of ochratoxin A in juice samples. *Talanta* **2018**, *188*, 225–231. [[CrossRef](#)]
117. Li, D.; Duan, H.; Ma, Y.; Deng, W. Headspace-sampling paper-based analytical device for colorimetric/surface-enhanced Raman scattering dual sensing of sulfur dioxide in wine. *Anal. Chem.* **2018**, *90*, 5719–5727. [[CrossRef](#)]
118. Picardo, M.; Filatova, D.; Nuñez, O.; Farré, M. Recent advances in the detection of natural toxins in freshwater environments. *TrAC-Trend. Anal. Chem.* **2019**, *112*, 75–86. [[CrossRef](#)]

119. Wu, Z.; Pu, H.; Sun, D.-W. Fingerprinting and tagging detection of mycotoxins in agri-food products by surface-enhanced Raman spectroscopy: Principles and recent applications. *Trends Food Sci. Tech.* **2021**, *110*, 393–404. [[CrossRef](#)]
120. Shao, B.; Ma, X.; Zhao, S.; Lv, Y.; Hun, X.; Wang, H.; Wang, Z. Nanogapped Au(core)@Au-Ag(shell) structures coupled with Fe<sub>3</sub>O<sub>4</sub> magnetic nanoparticles for the detection of Ochratoxin A. *Anal. Chim. Acta* **2018**, *1033*, 165–172. [[CrossRef](#)]
121. Rostami, S.; Zór, K.; Zhai, D.S.; Viehrig, M.; Morelli, L.; Mehdinia, A.; Smedsgaard, J.; Rindzevicius, T.; Boisen, A. High-throughput label-free detection of Ochratoxin A in wine using supported liquid membrane extraction and Ag-capped silicon nanopillar SERS substrates. *Food Control* **2020**, *113*, 107183. [[CrossRef](#)]
122. Wang, Q.; Liu, Y.; Bai, Y.; Yao, S.; Wei, Z.; Zhang, M.; Wang, L.; Wang, L. Superhydrophobic SERS substrates based on silver dendrite-decorated filter paper for trace detection of nitenpyram. *Anal. Chim. Acta* **2019**, *1049*, 170–178. [[CrossRef](#)] [[PubMed](#)]
123. Xie, T.; Cao, Z.; Li, Y.; Li, Z.; Zhang, F.L.; Gu, Y.; Han, C.; Yang, G.; Qu, L. Highly sensitive SERS substrates with multi-hot spots for on-site detection of pesticide residues. *Food Chem.* **2022**, *381*, 132208. [[CrossRef](#)] [[PubMed](#)]
124. Luo, J.; Wang, Z.; Li, Y.; Wang, C.; Sun, J.; Ye, W.; Wang, X.; Shao, B. Durable and flexible Ag-nanowire-embedded PDMS films for the recyclable swabbing detection of malachite green residue in fruits and fingerprints. *Sens. Actuat. B Chem.* **2021**, *347*, 130602. [[CrossRef](#)]
125. Ji, S.; Kou, S.; Wang, M.; Qiu, H.; Sun, X.; Dou, J.; Yang, Z. Two-step synthesis of hierarchical Ag/Cu<sub>2</sub>O/ITO substrate for ultrasensitive and recyclable surface-enhanced Raman spectroscopy applications. *Appl. Surf. Sci.* **2019**, *489*, 1002–1009. [[CrossRef](#)]
126. Ekmen, E.; Bilici, M.; Turan, E.; Tamer, U.; Zengin, A. Surface molecularly-imprinted magnetic nanoparticles coupled with SERS sensing platform for selective detection of malachite green. *Sens. Actuat. B Chem.* **2020**, *325*, 128787. [[CrossRef](#)]
127. Tang, S.; Li, Y.; Huang, H.; Li, P.; Guo, Z.; Luo, Q.; Wang, Z.; Chu, P.K.; Li, J.; Yu, X.F. Efficient enrichment and self-assembly of hybrid nanoparticles into removable and magnetic SERS substrates for sensitive detection of environmental pollutants. *ACS Appl. Mater. Interfaces* **2017**, *9*, 7472–7480. [[CrossRef](#)]
128. Lin, B.; Chen, J.; Zeng, Y.; Li, L.; Qiu, B.; Lin, Z.; Guo, L. A facile approach for on-site evaluation of nicotine in tobacco and environmental tobacco smoke. *ACS Sens.* **2019**, *4*, 1844–1850. [[CrossRef](#)]
129. Hu, R.; Tang, R.; Xu, J.; Lu, F. Chemical nanosensors based on molecularly-imprinted polymers doped with silver nanoparticles for the rapid detection of caffeine in wastewater. *Anal. Chim. Acta* **2018**, *1034*, 176–183. [[CrossRef](#)]
130. Li, H.; Wang, M.; Shen, X.; Liu, S.; Wang, Y.; Li, Y.; Wang, Q.; Che, G. Rapid and sensitive detection of enrofloxacin hydrochloride based on surface enhanced Raman scattering-active flexible membrane assemblies of Ag nanoparticles. *J. Environ. Manage.* **2019**, *249*, 109387. [[CrossRef](#)]
131. Berger, A.G.; Restaino, S.M.; White, I.M. Vertical-flow paper SERS system for therapeutic drug monitoring of flucytosine in serum. *Anal. Chim. Acta* **2017**, *949*, 59–66. [[CrossRef](#)] [[PubMed](#)]
132. Yu, S.; Liu, Z.; Wang, W.; Jin, L.; Xu, W.; Wu, Y. Disperse magnetic solid phase microextraction and surface enhanced Raman scattering (Dis-MSPME-SERS) for the rapid detection of trace illegally chemicals. *Talanta* **2018**, *178*, 498–506. [[CrossRef](#)] [[PubMed](#)]
133. Liu, J.; Si, T.; Zhang, Z. Mussel-inspired immobilization of silver nanoparticles toward sponge for rapid swabbing extraction and SERS detection of trace inorganic explosives. *Talanta* **2019**, *204*, 189–197. [[CrossRef](#)] [[PubMed](#)]
134. Cao, J.; Liu, H.L.; Yang, J.M.; Li, Z.Q.; Yang, D.R.; Ji, L.N.; Wang, K.; Xia, X.H. SERS detection of nucleobases in single silver plasmonic nanopores. *ACS Sens.* **2020**, *5*, 2198–2204. [[CrossRef](#)]
135. Huang, J.A.; Mousavi, M.Z.; Giovannini, G.; Zhao, Y.; Hubarevich, A.; Soler, M.A.; Rocchia, W.; Garoli, D.; De Angelis, F. Multiplexed discrimination of single amino acid residues in polypeptides in a single SERS hot spot. *Angew. Chem. Int. Ed.* **2020**, *59*, 11423–11431. [[CrossRef](#)]
136. Shen, Q.; Zhou, P.-L.; Huang, B.-T.; Zhou, J.; Liu, H.-L.; Ahmed, S.A.; Ding, X.-L.; Li, J.; Zhai, Y.-M.; Wang, K. Mass transport through a sub-10 nm single gold nanopore: SERS and ionic current measurement. *J. Electroanal. Chem.* **2021**, *894*, 115373. [[CrossRef](#)]
137. Hubarevich, A.; Huang, J.-A.; Giovannini, G.; Schirato, A.; Zhao, Y.; Maccaferri, N.; De Angelis, F.; Alabastri, A.; Garoli, D.  $\lambda$ -DNA through porous materials—Surface-enhanced Raman scattering in a simple plasmonic nanopore. *J. Phys. Chem. C* **2020**, *124*, 22663–22670. [[CrossRef](#)]
138. Chen, C.; Li, Y.; Kerman, S.; Neutens, P.; Willems, K.; Cornelissen, S.; Lagae, L.; Stakenborg, T.; Van Dorpe, P. High spatial resolution nanoslit SERS for single-molecule nucleobase sensing. *Nat. Commun.* **2018**, *9*, 733. [[CrossRef](#)]